

pubs.acs.org/acschemicalbiology Letters

A Nonfunctional Halogenase Masquerades as an Aromatizing Dehydratase in Biosynthesis of Pyrrolic Polyketides by Type I Polyketide Synthases

Dongqi Yi, Dhirendra Niroula, Will R. Gutekunst, Joyce E. Loper, Qing Yan, and Vinayak Agarwal*



Cite This: https://doi.org/10.1021/acschembio.2c00288



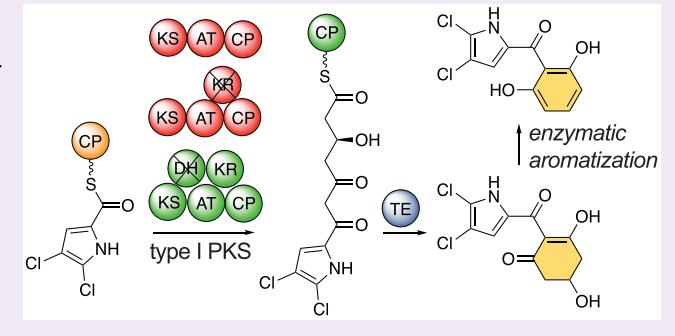
ACCESS I

Metrics & More

Article Recommendations

Supporting Information

ABSTRACT: The bacterial modular type I polyketide synthases (PKSs) typically furnish nonaromatic lactone and lactam natural products. Here, by the complete *in vitro* enzymatic production of the polyketide antibiotic pyoluteorin, we describe the biosynthetic mechanism for the construction of an aromatic resorcylic ring by a type I PKS. We find that the pyoluteorin type I PKS does not produce an aromatic product, rather furnishing an alicyclic dihydrophloroglucinol that is later enzymatically dehydrated and aromatized. The aromatizing dehydratase is encoded in the pyoluteorin biosynthetic gene cluster (BGC), and its presence is conserved in other BGCs encoding production of pyrrolic polyketides. Sequence similarity and mutational analysis demon-



strates that the overall structure and position of the active site for the aromatizing dehydratase is shared with flavin-dependent halogenases albeit with a loss in ability to perform redox catalysis. We demonstrate that the post-PKS dehydrative aromatization is critical for the antibiotic activity of pyoluteorin.

romatic polyketides are structurally diverse natural products with potent bioactivities. 1,2 Prominent examples include the tetracycline antibiotics, anticancer pharmaceutical doxorubicin, carcinogenic fungal aflatoxins, and plant flavonoids. Just as for all polyketides, the biosynthesis of aromatic polyketides is predicated upon a central thiotemplated poly- β ketone intermediate (Figure 1). This central intermediate is delivered by the repetitive decarboxylative Claisen condensation of malonyl-coenzyme A (malonyl-CoA) extender units by ketosynthases (KSs).^{3,4} Chain-extending KSs occur as catalytic domains embedded within PKSs or as standalone enzymes. The bacterial type II PKSs deliver poly- β -ketone intermediates acylated to carrier proteins (CPs) that are then cyclized, dehydrated, and aromatized by dedicated aromatase/cyclase (ARO/CYC) enzymes. For fungal nonreducing PKSs (nrPKSs), polyketide cyclization and aromatization are assisted by the product template (PT) and the Claisen cyclase/ thioesterase (CLC/TE) domains. The type III PKSs, typified by the plant chalcone synthase, deliver poly- β -ketone intermediates acylated to CoA with the iterative polyketide extension, cyclization, and aromatization all occurring within the KS active site (Figure 1).6

In contrast to the iterative bacterial type II PKSs, fungal nrPKSs, and plant type III PKSs, the modular assembly line-like type I PKSs typically yield macrolactone or macrolactam products.⁷ Typified by the assembly line biosynthesis of the erythromycin aglycone, the lactone (and lactam) formation is

catalyzed by the polyketide offloading thioesterase (TE) domain. Cyclization by Dieckmann cyclases can offload tetramic acid and pyridine products, among other offloading strategies leading to rich structural diversity.^{8,9}

With this background, it was interesting to note that the aromatic resorcylic ring in the natural product pyoluteorin (1, Figure 1) is furnished by type I PKSs encoded within the *plt* BGC in the bacterium *Pseudomonas protegens* Pf-5. ^{10,11} The *plt* BGC does not encode any ARO/CYC, PT, or Dieckmann cyclases. Instead, a standalone type II TE, PltG, is encoded within the *plt* BGC. The absence of genes encoding enzymes that participate in the cyclization and aromatizing dehydration reactions in type II PKS and nrPKS-derived natural products was also noteworthy in the BGCs for other pyrrolic polyketide natural products such as the marinopyrroles, ¹² pyrrolomycins, ¹³ and pyralomicins ¹⁴ that likewise contain phenol and resorcylic rings appended to the aromatic pyrrole via a bridging carbonyl. Here, we asked how an assembly line type I PKS constructed the resorcylic ring in 1 and if any additional

Received: April 4, 2022 Accepted: June 2, 2022



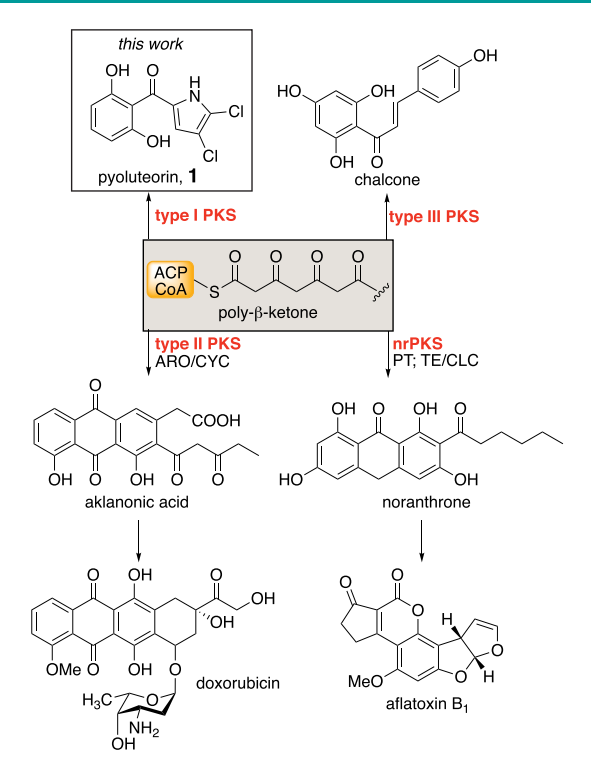


Figure 1. Biosynthesis of aromatic polyketides.

unknown enzymes participated in this biosynthetic transformation.

To query the mechanism for the construction of the resorcylic ring in 1, we attempted the total in vitro biosynthesis of 1 using purified enzymes. We have previously described the organization of the plt BGC encoding production of 1 (Figure 2A). The domain organization of the modular type I PKSs PltB and PltC is illustrated in Figure 2B. The ATP-dependent malonyl-CoA synthetase MatB was employed in situ to generate malonyl-CoA substrate for the PltB and PltC acyltransferase (AT) domains (Figure 2C). 15 Similarly, phosphite dehydrogenase PtdH was used to regenerate NADPH required to support the activity of the PltC ketoreductase (KR) domain. 16 Biosynthetic construction of the initiator substrate, dichloropyrrole thiotemplated to the CP PltL, is well established.¹⁷ In this study, dichloropyrrolyl-S-PltL was accessed using a chemoenzymatic strategy which involved the ATP-dependent extension of synthetic dichloropyrrolyl-Spantetheine to dichloropyrrolyl-S-CoA coupled with the enzymatic transfer of the acyl-phosphopantetheine to apo-PltL (Figure S1). 18 To facilitate recombinant protein production, the bimodular PKS PltB was separated into two peptides each containing one PKS module. To facilitate the productive assembly of the otherwise covalently linked PltB modules in vitro, docking domains from the 6-deoxyerythronolide B synthase (DEBS) were appended to the separated PltB modules (Table S1). 19

Upon incubation of reaction components, 1 was not produced. Rather, we observed the production of a metabolite with mass corresponding to a hydrated derivative of 1. Production of this metabolite was abolished in the absence of the PKSs (Figure S2). Spectroscopic characterization established the structure as 2 (Figure 2B and Figures S3–S6, Tables S2–S3), wherein the γ -resorcylic ring of 1 was replaced by a dihydrophloroglucinol. The Dieckmann condensation activity

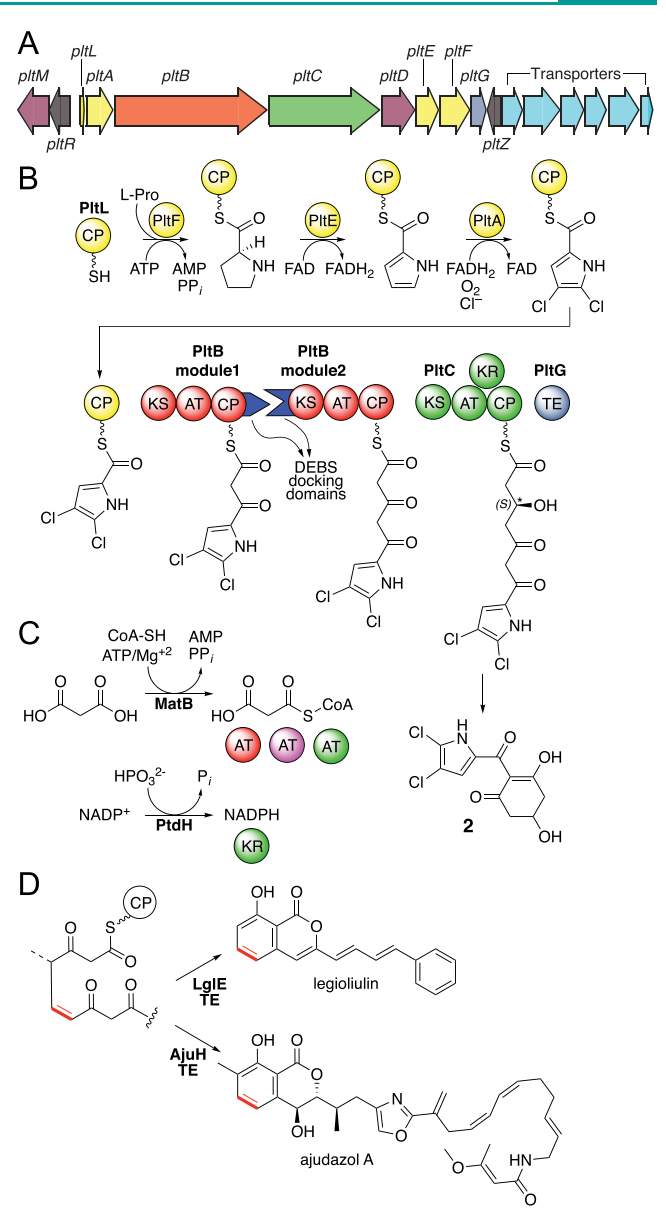


Figure 2. Plt PKSs. (A) The plt BGC. Genes pltR and pltZ encode transcriptional regulators. (B) Construction of compound 2. The adenyltransferase PltF, oxidase PltE, and halogenase PltA participate in the biosynthesis of dichloropyrrolyl-S-PltL. Pks. PltB and PltC domain organization and inferred polyketide extension steps leading to 2. Docking domains from the DEBS PKS that were appended to the PltB PKS modules are represented as blue wedges. The PltB module2 and PltC PKS harbor inactive KR and DH domains, respectively (Figures S7 and S8). Stereochemistry at the secondary alcohol (*) is inferred from the PltC KR sequence (Figure S7); the dihydrophloroglucinol ring is racemized through keto—enol tautomerization. (C) Malonyl-CoA and NADPH regeneration systems employed in the polyketide extension reaction. (D) Inferred functions of LglE and AjuH type II TE domains.

of the standalone type II TE PltG mirrors that of other type II TEs embedded within terminal modules of type I PKSs LglE and AjuH that participate in coumarin ring synthesis in legioliulin and ajudazols, respectively (Figure 2D). However, unlike the inactive dehydratase (DH) domain in PKS PltC, 10 LglE and AjuH TE domains are preceded by functional DH domains in their respective PKS modules. A functional PltC DH domain would conceivably allow for

offloading of resorcylic 1 from the PltC CP, rather than the dihydrophloroglucinol 2.

Dihydrophloroglucinol-containing natural products have been isolated from a *Nodulisporium* sp. fungus, ²⁴ in addition to their production by enzymatic reduction of phloroglucinols. ²⁵ As such, an extended incubation of **2** did not afford spontaneous aromatization to **1** (Figure S9). Instead, addition of the total protein extract from *P. protegens* Pf-5 to the polyketide extension reaction led to the production of **1**. However, addition of protein extracts from other Pseudomonads that do not produce **1** did not recover the production of **1** (Figure S10). Hence, we hypothesized that an additional enzyme encoded in the *plt* BGC, which would be present in the *P. protegens* Pf-5 proteome but not in other Pseudomonad proteomes was required for the production of **1**.

Apart from the transcriptional regulators encoded by genes pltR and pltZ²⁶ and transporters encoded in the plt BGC (Figure 2B), each enzyme encoded in the plt BGC was recombinantly produced. Only upon the addition of PltD to the Plt PKS assay did we recover the production of 1 (Figure 3A). Incubation of 2 alone with PltD also produced 1 with kinetic parameters $k_{\rm cat}$ 1.7 \pm 0.08 min⁻¹ and $K_{\rm M}$ 258 \pm 24 $\mu{\rm M}$ (Figure S11). To corroborate the in vitro conversion of 2 to 1 by PltD, we deleted the pltD gene in P. protegens Pf-5 and observed the accumulation of 2 in the culture extracts, together with the absence of 1 (Figure 3B). Upon reintroduction of the pltD gene, the production of 1 recovered. These data demonstrate that the physiological product of the Plt PKSs is the dihydrophloroglucinol 2 and not the resorcylic 1, and that the enzyme PltD is required for the dehydration and aromatization of 2 to 1.

Compound **1**, produced by the soil dwelling bacterium *P. protegens* Pf-5, possesses potent antibiotic activity against a number of plant pathogens including the fire blight causing bacterium *Erwinia amylovora*.²⁷ Antibiotic activity against *E. amylovora* is predicated upon post-PKS tailoring of **2** by PltD; we found **2** to be significantly less bioactive than **1** (Figure 3C, Figure S12). PltD homologues are present in biosynthetic gene clusters encoding production of other pyrrolic polyketide antibiotics as well (Figure S13).

The PltD catalyzed transformation resembles the dehydrative aromatization reactions catalyzed by ARO/CYC enzymes that partner with type II PKSs for the production of aromatic polyketides (Figure S14).4 However, PltD and similar enzymes encoded in BGCs for other pyrrolic polyketides are annotated as nonfunctional flavin-dependent halogenases (FDHs). 12,13,23 The primary sequence of PltD is indeed similar to that of FDHs with the most similar structurally characterized enzyme being the phloroglucinol chlorinase PltM (Figure 4A, Figure S15).²⁸ PltD and PltM are encoded within the same plt BGC (Figure 2A). PltM products, the chlorophloroglucinols, activate expression of the plt BGC.²⁹ PltD lacks sequence motifs required for binding flavin (Figure S16); recombinant PltD did not bind flavin and the flavin cofactor was not required for the conversion of 2 to 1 (Figure S17). Unlike other flavin-dependent enzymes encoded within the plt BGC, PltD did not participate in proline oxidation or pyrrole halogenation (Figures S18 and S19). Indeed, the cofactor-independent redox-neutral dehydration catalyzed by PltD is distinct from that of oxidative halogenation reactions catalyzed by FDHs³⁰ and is reminiscent of hydronitrile lyases where the bystander flavin only plays a structural role.31,32 What is then the rationale and possible

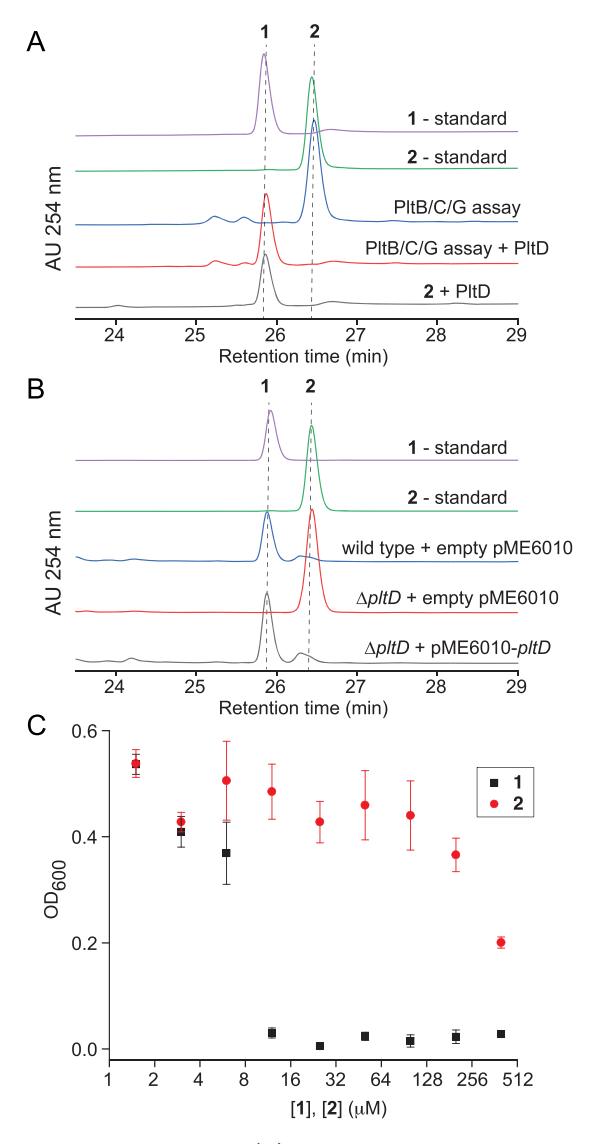


Figure 3. PltD activity. (A) UV-absorbance chromatograms demonstrating that the addition of PltD to the polyketide synthesis reaction (labeled as the "PltB/C/G assay"; illustrated in Figure 2B) yielded 1, as did the incubation of 2 with PltD. (B) Deletion of pltD gene abolished production of 1 in P. protegens Pf-5 and accumulated 2. Upon reintroduction of the pltD gene using the pME6010 plasmid, production of 1 was restored. (C) Growth of plant pathogen E. amylovora monitored by optical density at 600 nm (OD₆₀₀) upon addition of 1 and 2. Means from four replicates of an experiment which was repeated thrice independently are reported with error bars representing the standard deviation.

mechanistic implications for the resemblance of PltD to FDHs?

For FDHs, only the first half reaction involves redox transformation of the halide to a halonium. The second half reaction for FDHs proceeds via redox neutral acid/base catalysis. Here, the electrophilic aromatic substitution using the halonium is assisted by a glutamate residue which was proposed to act as a catalytic base to facilitate rearomatization of the Wheland intermediate for indolic substrates.³³ Active site amino acid side chains facilitating acid/base catalyzed aldol cyclization and dehydration reactions are implicated in bacterial type II PKS ARO/CYC enzymes as well.^{34–36}

For FHDs such as PltM, a catalytic lysine residue (K87 for PltM, Figure 4A) facilitates halonium transfer from the redox

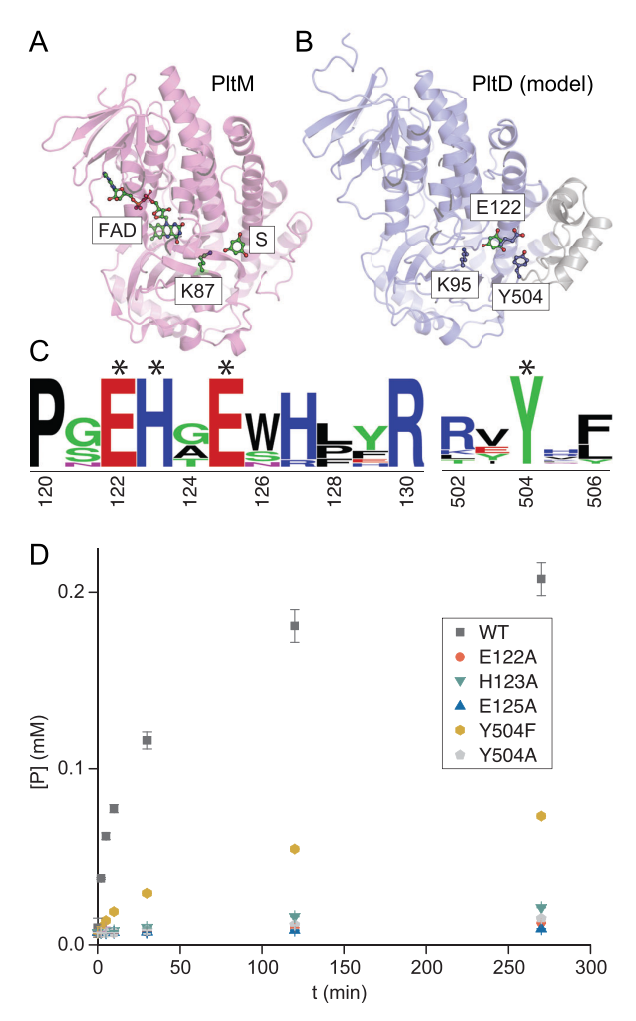


Figure 4. PltD active site. (A) PltM structure with flavin (FAD) and phloroglucinol (S) binding sites labeled along with the catalytic lysine residue (K87). (B) Homology structure of PltD with the substrate from the PltM structure overlaid to identify a putative substrate binding site. (C) PltD sequence alignment identifies conservation of residues in the vicinity of the hypothetical PltD substrate binding site (see Table S4 for sequences included). Residues targeted for mutagenesis are marked with (*). (D) Activity of wild type and mutant PltD enzymes monitored by product (1) formation over time.

active site (proximal to the flavin) to the substrate binding site (marked "S" in Figure 4A). ^{28,30} Mutation at this lysine residue leads to loss of halogenating activity for all FDHs. Mutating the corresponding lysine residue for PltD (K95, Figure 4B) to an alanine led to no change in PltD activity (Figure S20). The substrate binding site for PltM was overlaid upon the PltD modeled structure. In the vicinity of the thusly identified *hypothetical* PltD active site were discerned several highly conserved amino acid residues that could potentially participate in acid/base catalysis, such as E122 and Y504 (Figure 4B,C). Mutation of these residues compromised PltD activity (Figure 4D), allowing us to posit that PltD shares the dihydrophloroglucinol substrate binding site with the phloroglucinol binding site of PltM.

The discovery of new tailoring enzymes that participate in the construction of polyketide antibiotics has traditionally relied on *in vivo* gene deletion experiments in native or heterologous hosts, the detection and isolation of biosynthetic intermediates, and assignment of the tailoring enzyme activities

by gene complementation and model or native in vitro reactions. Specific to the production of aromatic polyketides, reminiscent here are the studies implicating the participation of NAD(P)(H)-dependent short chain dehydrogenases/reductases in catalyzing or facilitating polyketide cyclization/ aromatization reactions.^{37,38} Complementary to in vivo gene manipulation experiments, the total in vitro reconstitution of large modular type I PKSs is now accessible which enables the discovery of new polyketide natural products and polyketide assembly line engineering.^{39–41} Here, we employ the total *in* vitro reconstitution of the type I PKSs to discover a novel post-PKS tailoring enzymatic activity. We demonstrate that the Plt PKSs themselves produce a biologically inactive alicyclic dihydrophloroglucinol polyketide product, a chemical class of products previously not reported to be produced by type I PKSs. This polyketide product is later dehydratively aromatized to the biologically active aromatic polyketide in an enzymatic reaction that is completely untied to the modular polyketide chain extension. Using a combination of biochemical assays and genetic manipulations, we identify the enzyme PltD to be responsible for this transformation. The enzyme PltD has borrowed the overall architecture from FDHs and dispensed with the ability to bind flavin and perform redox catalysis, but the substrate binding site is preserved and tailored to perform a highly specialized post-PKS tailoring modification in pyrrolic polyketide biosynthesis. The reaction catalyzed by PltD makes it an attractive biotechnology tool to explore the enzymatic conversion of dihydrophloroglucinol substrates to aromatic resorcylic products.

ASSOCIATED CONTENT

Solution Supporting Information

The Supporting Information is available free of charge at https://pubs.acs.org/doi/10.1021/acschembio.2c00288.

Experimental details for recombinant protein production, polyketide production reactions, analytical procedures for compound characterization, bioactivity assays, and additional characterization data and spectra (PDF)

AUTHOR INFORMATION

Corresponding Author

Vinayak Agarwal — School of Chemistry and Biochemistry and School of Biological Sciences, Georgia Institute of Technology, Atlanta, Georgia 30332, United States; orcid.org/0000-0002-2517-589X; Phone: (+1)404-385-3798; Email: vagarwal@gatech.edu

Authors

Dongqi Yi — School of Chemistry and Biochemistry, Georgia Institute of Technology, Atlanta, Georgia 30332, United States

Dhirendra Niroula — Department of Plant Sciences and Plant Pathology, Montana State University, Bozeman, Montana 59717, United States

Will R. Gutekunst — School of Chemistry and Biochemistry and School of Materials Science and Engineering, Georgia Institute of Technology, Atlanta, Georgia 30332, United States

Joyce E. Loper – Department of Botany and Plant Pathology, Oregon State University, Corvallis, Oregon 97331, United States; USDA-Agricultural Research Service, Corvallis, Oregon 97330, United States

Qing Yan — Department of Plant Sciences and Plant Pathology, Montana State University, Bozeman, Montana 59717, United States; Department of Botany and Plant Pathology, Oregon State University, Corvallis, Oregon 97331, United States

Complete contact information is available at: https://pubs.acs.org/10.1021/acschembio.2c00288

Notes

The authors declare no competing financial interest.

ACKNOWLEDGMENTS

The authors acknowledge support from the NSF (Grant CHE-2004030) and the NIH (Grant GM142882) to V.A. The authors thank N. Garg for the *Pseudomonas* strains, B. Palfey for insightful discussions, and X. Sui for assistance with the NMR data acquisition and analysis.

REFERENCES

- (1) Das, A.; Khosla, C. Biosynthesis of aromatic polyketides in bacteria. *Acc. Chem. Res.* **2009**, 42 (5), 631–639.
- (2) Crawford, J. M.; Townsend, C. A. New insights into the formation of fungal aromatic polyketides. *Nat. Rev. Microbiol* **2010**, 8 (12), 879–889.
- (3) Hertweck, C. The biosynthetic logic of polyketide diversity. *Angew. Chem., Int. Ed. Engl.* **2009**, 48 (26), 4688–716.
- (4) Tsai, S.-C. The structural enzymology of iterative aromatic polyketide synthases: a critical comparison with fatty acid synthases. *Annu. Rev. Biochem.* **2018**, *87* (1), 503–531.
- (5) Chooi, Y.-H.; Tang, Y. Navigating the fungal polyketide chemical space: from genes to molecules. *J. Org. Chem.* **2012**, *77* (22), 9933–9953.
- (6) Abe, I.; Morita, H. Structure and function of the chalcone synthase superfamily of plant type III polyketide synthases. *Nat. Prod Rep* **2010**, 27 (6), 809–838.
- (7) Weissman, K. J. 1.02 Bacterial type I polyketide synthases. In *Comprehensive Natural Products III*; Liu, H.-W., Begley, T. P., Eds.; Elsevier: Oxford, U.K., 2020; pp 4–46.
- (8) Adrover-Castellano, M. L.; Schmidt, J. J.; Sherman, D. H. Biosynthetic cyclization catalysts for the assembly of peptide and polyketide natural products. *ChemCatChem.* **2021**, *13* (9), 2095–2116.
- (9) Little, R. F.; Hertweck, C. Chain release mechanisms in polyketide and non-ribosomal peptide biosynthesis. *Nat. Prod Rep* **2022**, 39 (1), 163–205.
- (10) Nowak-Thompson, B.; Gould, S. J.; Loper, J. E. Identification and sequence analysis of the genes encoding a polyketide synthase required for pyoluteorin biosynthesis in *Pseudomonas fluorescens* Pf-5. *Gene* 1997, 204 (1), 17–24.
- (11) Nowak-Thompson, B.; Chaney, N.; Wing, J. S.; Gould, S. J.; Loper, J. E. Characterization of the pyoluteorin biosynthetic gene cluster of *Pseudomonas fluorescens* Pf-5. *J. Bacteriol.* **1999**, *181* (7), 2166–74.
- (12) Yamanaka, K.; Ryan, K. S.; Gulder, T. A.; Hughes, C. C.; Moore, B. S. Flavoenzyme-catalyzed atropo-selective N,C-bipyrrole homocoupling in marinopyrrole biosynthesis. *J. Am. Chem. Soc.* **2012**, 134 (30), 12434—7.
- (13) Zhang, X.; Parry, R. J. Cloning and characterization of the pyrrolomycin biosynthetic gene clusters from *Actinosporangium vitaminophilum* ATCC 31673 and *Streptomyces* sp. strain UC 11065. *Antimicrob. Agents Chemother.* **2007**, *51* (3), 946–57.
- (14) Flatt, P. M.; Wu, X.; Perry, S.; Mahmud, T. Genetic insights into pyralomicin biosynthesis in *Nonomuraea spiralis* IMC A-0156. *J. Nat. Prod* **2013**, *76* (5), 939–946.
- (15) Hughes, A. J.; Keatinge-Clay, A. Enzymatic extender unit generation for in vitro polyketide synthase reactions: structural and

- functional showcasing of Streptomyces coelicolor MatB. Chem. Biol. 2011, 18 (2), 165-76.
- (16) Johannes, T. W.; Woodyer, R. D.; Zhao, H. Efficient regeneration of NADPH using an engineered phosphite dehydrogenase. *Biotechnol. Bioeng.* **2007**, *96* (1), 18–26.
- (17) Jaremko, M. J.; Davis, T. D.; Corpuz, J. C.; Burkart, M. D. Type II non-ribosomal peptide synthetase proteins: structure, mechanism, and protein-protein interactions. *Nat. Prod. Rep.* **2020**, *37*, 355.
- (18) Yi, D.; Acharya, A.; Gumbart, J. C.; Gutekunst, W. R.; Agarwal, V. Gatekeeping ketosynthases dictate initiation of assembly line biosynthesis of pyrrolic polyketides. *J. Am. Chem. Soc.* **2021**, *143* (20), 7617–7622.
- (19) Broadhurst, R. W.; Nietlispach, D.; Wheatcroft, M. P.; Leadlay, P. F.; Weissman, K. J. The structure of docking domains in modular polyketide synthases. *Chem. Biol.* **2003**, *10* (8), 723–731.
- (20) Buntin, K.; Weissman, K. J.; Muller, R. An unusual thioesterase promotes isochromanone ring formation in ajudazol biosynthesis. *Chembiochem* **2010**, *11* (8), 1137–46.
- (21) Ahrendt, T.; Miltenberger, M.; Haneburger, I.; Kirchner, F.; Kronenwerth, M.; Brachmann, A. O.; Hilbi, H.; Bode, H. B. Biosynthesis of the natural fluorophore legioliulin from *Legionella*. *Chembiochem* **2013**. *14* (12), 1415–8.
- (22) Thomas, M. G.; Burkart, M. D.; Walsh, C. T. Conversion of L-proline to pyrrolyl-2-carboxyl-S-PCP during undecylprodigiosin and pyoluteorin biosynthesis. *Chem. Biol.* **2002**, *9* (2), 171–84.
- (23) Dorrestein, P. C.; Yeh, E.; Garneau-Tsodikova, S.; Kelleher, N. L.; Walsh, C. T. Dichlorination of a pyrrolyl-S-carrier protein by FADH2-dependent halogenase PltA during pyoluteorin biosynthesis. *Proc. Natl. Acad. Sci. U. S. A.* **2005**, *102* (39), 13843–8.
- (24) Igarashi, M.; Tetsuka, Y.; Mimura, Y.; Takahashi, A.; Tamamura, T.; Sato, K.; Naganawa, H.; Takeuchi, T. AB5046A and B, novel chlorosis-inducing substances from *Nodulisporium* sp. *J. Antibiot (Tokyo)* 1993, 46 (12), 1843–8.
- (25) Conradt, D.; Hermann, B.; Gerhardt, S.; Einsle, O.; Muller, M. Biocatalytic properties and structural analysis of phloroglucinol reductases. *Angew. Chem., Int. Ed. Engl.* **2016**, *55* (50), 15531–15534.
- (26) Yan, Q.; Liu, M.; Kidarsa, T.; Johnson, C. P.; Loper, J. E. Two pathway-specific transcriptional regulators, PltR and PltZ, coordinate autoinduction of pyoluteorin in *Pseudomonas protegens* Pf-5. *Microorganisms* **2021**, 9 (7), 1489.
- (27) Bender, C. L.; Rangaswamy, V.; Loper, J. Polyketide production by plant-associated Pseudomonads. *Ann. Rev. Phytopathol* **1999**, 37 (1), 175–196.
- (28) Mori, S.; Pang, A. H.; Thamban Chandrika, N.; Garneau-Tsodikova, S.; Tsodikov, O. V. Unusual substrate and halide versatility of phenolic halogenase PltM. *Nat. Commun.* **2019**, *10* (1), 1255.
- (29) Yan, Q.; Philmus, B.; Chang, J. H.; Loper, J. E. Novel mechanism of metabolic co-regulation coordinates the biosynthesis of secondary metabolites in *Pseudomonas protegens*. *eLife* **2017**, *6*, No. e22835.
- (30) Crowe, C.; Molyneux, S.; Sharma, S. V.; Zhang, Y.; Gkotsi, D. S.; Connaris, H.; Goss, R. J. M. Halogenases: a palette of emerging opportunities for synthetic biology-synthetic chemistry and C-H functionalisation. *Chem. Soc. Rev.* **2021**, *50* (17), 9443–9481.
- (31) Bornemann, S. Flavoenzymes that catalyse reactions with no net redox change. *Nat. Prod Rep* **2002**, *19* (6), 761–772.
- (32) Dreveny, I.; Andryushkova, A. S.; Glieder, A.; Gruber, K.; Kratky, C. Substrate binding in the FAD-dependent hydroxynitrile lyase from almond provides insight into the mechanism of cyanohydrin formation and explains the absence of dehydrogenation activity. *Biochemistry* **2009**, *48* (15), 3370–3377.
- (33) Dong, C.; Flecks, S.; Unversucht, S.; Haupt, C.; van Pee, K. H.; Naismith, J. H. Tryptophan 7-halogenase (PrnA) structure suggests a mechanism for regioselective chlorination. *Science* **2005**, *309* (5744), 2216–9.
- (34) Ames, B. D.; Lee, M.-Y.; Moody, C.; Zhang, W.; Tang, Y.; Tsai, S.-C. Structural and biochemical characterization of ZhuI aromatase/

cyclase from the R1128 polyketide pathway. *Biochemistry* **2011**, *50* (39), 8392–8406.

- (35) Caldara-Festin, G.; Jackson, D. R.; Barajas, J. F.; Valentic, T. R.; Patel, A. B.; Aguilar, S.; Nguyen, M.; Vo, M.; Khanna, A.; Sasaki, E.; Liu, H.-w.; Tsai, S.-C. Structural and functional analysis of two didomain aromatase/cyclases from type II polyketide synthases. *Proc. Natl. Acad. Sci. U. S. A.* **2015**, *112* (50), No. E6844.
- (36) Lee, M.-Y.; Ames, B. D.; Tsai, S.-C. Insight into the molecular basis of aromatic polyketide cyclization: crystal structure and in vitro characterization of WhiE-ORFVI. *Biochemistry* **2012**, *51* (14), 3079–3091.
- (37) Gao, Y.; Zhao, Y.; Zhou, J.; Yang, M.; Lin, L.; Wang, W.; Tao, M.; Deng, Z.; Jiang, M. Unexpected role of a short-chain dehydrogenase/reductase family protein in type II polyketide biosynthesis. *Angew. Chem., Int. Ed. Engl.* **2022**, 61 (7), No. e202110445.
- (38) Liu, L.; Tang, M.-C.; Tang, Y. Fungal highly reducing polyketide synthases biosynthesize salicylaldehydes that are precursors to epoxycyclohexenol natural products. *J. Am. Chem. Soc.* **2019**, *141* (50), 19538–19541.
- (39) Yuet, K. P.; Liu, C. W.; Lynch, S. R.; Kuo, J.; Michaels, W.; Lee, R. B.; McShane, A. E.; Zhong, B. L.; Fischer, C. R.; Khosla, C. Complete reconstitution and deorphanization of the 3 MDa nocardiosis-associated polyketide synthase. *J. Am. Chem. Soc.* **2020**, 142 (13), 5952–5957.
- (40) Miyazawa, T.; Hirsch, M.; Zhang, Z.; Keatinge-Clay, A. T. An *in vitro* platform for engineering and harnessing modular polyketide synthases. *Nat. Commun.* **2020**, *11* (1), 80.
- (41) Lowry, B.; Robbins, T.; Weng, C.-H.; O'Brien, R. V.; Cane, D. E.; Khosla, C. In vitro reconstitution and analysis of the 6-deoxyerythronolide B synthase. *J. Am. Chem. Soc.* **2013**, *135* (45), 16809–16812.



SUPPLEMENTARY INFORMATION FOR:

A non-functional halogenase masquerades as an aromatizing dehydratase in biosynthesis of pyrrolic polyketides by type I polyketide synthases

Dongqi Yi,¹ Dhirendra Niroula,² Will R. Gutekunst,¹,³ Joyce E. Loper,⁴,⁵ Qing Yan,²,⁴ Vinayak Agarwal¹,6,*

¹School of Chemistry and Biochemistry, Georgia Institute of Technology, Atlanta GA, USA 30332

²Department of Plant Sciences and Plant Pathology, Montana State University, Bozeman MT, USA 59717

³School of Materials Science and Engineering, Georgia Institute of Technology, Atlanta GA, USA 30332

⁴Department of Botany and Plant Pathology, Oregon State University, Corvallis OR, USA 97331

⁵USDA-Agricultural Research Service, Corvallis OR, USA 97330

⁶School of Biological Sciences, Georgia Institute of Technology, Atlanta GA, USA 30332

*Correspondence: vagarwal@gatech.edu; Ph: (+1)404-385-378

Supplementary Information document contains:

Supplementary Methods

Supplementary Tables 1–4

Supplementary Figures S1–S20

Supplementary References

SUPPLEMENTARY METHODS

General procedures

All chemicals, solvents and media components were obtained commercially from Sigma-Aldrich, Fisher Scientific, and Alfa Aesar, and used without further purification. Silica gel (60, particle size 0.036-0.071 mm) was used for flash chromatography. ^{1}H and ^{13}C NMR spectra was recorded on Bruker Avance IIIHD 500 and 700 MHz instruments in CDCl₃ (contains 0.03% (v/v) TMS) and calibrated using residual undeuterated solvent as internal reference (δ_{H} 7.26 and δ_{C} 77.16). The splitting patterns were reported as s=singlet, d=doublet, t=triplet. High resolution mass spectrometry (MS) data was collected on an Agilent 1290 Infinity II UHPLC system coupled to a Bruker impact II Q-ToF mass spectrometer operating at room temperature in the negative ionization mode.

Cloning, expression and purification of holo-PltB M1, holo-PltB M2 and holo-PltC

PltB module1 with DEBS2 docking domain as well as module2 with DEBS3 docking domain (sequences shown in Table S1) cloned for expression in the pET28(+) vector were synthesized and provided by Twist Biosciences. The DNA fragments encoding PltC were amplified from the genomic DNA purified from *Pseudomonas protegens* Pf-5 using Phusion high-fidelity DNA polymerase and cloned into pET24(+) vector using Gibson assembly protocols. Sfp in the MCS1 of pCDFDuet-1 vector was constructed as previously described.¹

For overexpression of phosphopantetheinyl modified PKSs, two plasmids carrying PKS modules and Sfp were co-transformed into *Escherichia coli* BL21Gold(DE3). Overnight seed culture was inoculated in 1 L terrific broth media supplemented with appropriate antibiotics and D-pantothenic acid (15 mg/L). The cells were grown at 30 °C until OD₆₀₀ reached 0.4–0.5 at which time the incubation temperature was reduced to 18 °C. When OD₆₀₀ reached 0.7–0.8, bacterial cell cultures were induced by the addition of 0.05 mM IPTG and grown at 18 °C for an addition of 18 h. All subsequent steps of protein purification were performed at 4 °C or on ice. Cells were harvested by centrifugation (5,000 rpm, 20 min), resuspended in binding buffer (20 mM Tris-HCl (pH=8.0), 500 mM NaCl, 10% glycerol) and lysed by sonication (15 s sonication, 45 s off per circle). The lysate was clarified by centrifugation (18,000 rpm, 45 min), applied to a 5 mL HisTrap HP column using ÄKTAprime plus FPLC system. The column was washed extensively with wash buffer (20 mM Tris-HCl (pH=8.0), 30 mM imidazole, 500 mM NaCl, 10% glycerol), and then eluted with a linear gradient to 100 % of elution buffer (20 mM Tris-HCl (pH=8.0), 250 mM imidazole, 500 mM NaCl, 10% glycerol) over 8 column volumes. Purity of eluent fractions were checked by SDS-PAGE. The fractions containing desired proteins were pooled, concentrated using 50 kDa Amicon

centrifugal filters, and desalted into binding buffer with PD-10 columns. Purified proteins were stored as small aliquots at -80 °C and fresh aliquots were used each time for enzyme assays.

Cloning, expression, and purification of PltG, PltD and other enzymes.

MatB and PtdH enzymes were obtained as previously described.²⁻³ The DNA fragment encoding PltG was synthesized by Twist Biosciences and used as a template for PCR with Phusion high-fidelity DNA polymerase. The amplified *pltG* gene was then cloned into pET24(+) vector using Gibson assembly. The DNA fragment containing *pltD* gene was first amplified from the genomic DNA of *P. protegens* Pf-5 with forward primer (CTGGCCCGTTCGATAAAGGA) and reverse primer (GCGAGTGTTCATTGCCAC) using PrimeSTAR DNA polymerase, and then used as template for PCR. The amplified gene fragment encoding PltD was assembled into pET28(+)-MBP vector which contains a N-terminal His₆ tag followed by maltose-binding protein (MBP) using Gibson assembly. Plasmids for PltD mutants were generated by site-directed mutagenesis using primers containing desired mutations. Expression plasmids were transformed into *E. coli* BL21Gold(DE3). The bacterial cell cultures were grown in 1 L terrific broth medium supplemented with appropriate antibiotics at 30 °C until OD₆₀₀ reached 0.4–0.5. Then, temperature was reduced to 18 °C. When OD₆₀₀ reached 0.7–0.8, protein expression was induced by the addition of 0.2 mM IPTG. The induced cultures were grown at 18 °C for an addition of 18 h. Enzymes were purified following similar procedures described for *holo*-PKSs, except that PltG was concentrated with 10 kDa Amicon centrifugal filters, while PltD was concentrated with 30 kDa Amicon centrifugal filters.

In vitro reconstitution of pyoluteorin assembly line

The starting substrate for the polyketide extension reaction, dichloro-pyrrolyl-*S*-PltL was prepared as previously described.¹ PKS assays were performed in a total volume of 500 μL containing malonyl-CoA regenerating system (5 mM malonate, 1 mM coenzyme A, 5 mM ATP, 10 mM MgCl₂, and 6 μM MatB), NADPH regenerating system (4 mM Na₂HPO₃, 1 mM NADP⁺, 4 μM PtdH), 5 mM TCEP, 50 μM dichloro-pyrrolyl-*S*-PltL, 5 μM *holo*-PltB module1, 5 μM *holo*-PltB module2, 5 μM *holo*-PltC, 5 μM PltG, 0 or 8 μM PltD, and 400 mM potassium phosphate buffer (pH=7.5). The enzyme assays were incubated at 30 °C for 3 h, quenched, and extracted using EtOAc (500 μL, 3×). The organic layers were combined and concentrated under vacuum. The extracts were then reconstituted in 200 μL MeOH, 30 μL of which was injected for HPLC analysis.

HPLC analysis for detection of 1 and 2

HPLC analysis to monitor the production of **1** and **2** was carried out on Luna 5 μ m C8(2) 100 Å LC column (250×4.6 mm) using Agilent 1260 Infinity HPLC system. Water (solvent A) and MeCN (solvent B) with 0.1 % TFA were used as the mobile phase. A flow rate of 0.5 mL·min⁻¹ was used with the following gradient: 0-5 min: 5% B, 5-30 min: linear gradient to 100% B, 30-34 min: 100% B, 34-35 min: linear gradient to 5% B, 35-36 min: 5 % B, 36-37 min: linear gradient to 100% B, 37-38 min: 100% B, 38-39 min: linear gradient to 5% B. UV-absorbance was monitored at 254 and 280 nm.

Generation of protein extracts from Pseudomonas strains

P. protegens Pf-5, *P. aeruginosa* PAO1 and *P. aeruginosa* PA14 strains were inoculated in 50 mL LB media from glycerol stocks and grown at 30 °C overnight. Cells were harvested by centrifugation (6,000 rpm, 30 min), resuspended in 15 mL binding buffer, and lysed by sonication (10 s sonication, 50 s off per circle). The lysate was clarified by centrifugation (18,000 rpm, 50 min) and dialyzed in 1 L binding buffer for 7.5 h, during which the dialysis buffer was changed every 1.5 hours. After dialysis, protein extracts were added to polyketide extension assays (final concentration of protein extract in assays was 18% v/v), and the assays were incubated at 30 °C overnight before extraction by EtOAc following the same protocol described above.

Construction of P. protegens Pf-5 \(\Delta pltD \) mutant and its complementation

The deletion and complementation experiments were performed by following our previous method.⁴ The $\Delta pltD$ mutant was made by deleting pltD from the chromosome of the wild type P. protegens Pf-5. Briefly, a 1674 bp DNA fragment containing the wild type pltD gene was PCR amplified using oligonucleotides pltD (TAGGTACCCATGATCTGTGATTGAGGTGG), and

pltDr (TATAAGCTTCAACTCTCCTTGCGCAGGG).

The PCR product was digested by KpnI and HindIII and ligated in pEX18Tc to make a construct p18Tc-pltD which served as template DNA in a PCR reaction using oligonucleotides pltD-delete-F1 (ATCTGCAGTGACCCAGCGCCCCAG) and pltD-delete-R1 (ATGCCTTCGCCCGTGTCTGGCTG). The PCR product was digested by PstI and self-ligated to remove a 697 bp fragment in the frame of *pltD*. The resultant construct p18Tc-ΔpltD was transferred into the wild type Pf-5 to delete *pltD* in the chromosome. The deletion of *pltD* was confirmed by PCR and subsequent DNA sequencing.

To complement the $\Delta pltD$ mutant, the 1674 bp DNA fragment containing the wild type pltD gene amplified by pltDf and pltDr was digested with KpnI and HindIII and ligated in pME6010 to make the complementation construct pME6010-pltD. The empty vector pME6010 and the complementation construct pME6010-pltD were then transferred into the $\Delta pltD$ mutant.

Organic extraction of P. protegens Pf-5 strains

Organic extraction of *P. protegens* Pf-5 wild type with empty pME6010 vector, $\Delta pltD$ with empty vector and $\Delta pltD$ with pME6010-pltD were conducted following the same protocol. *P. protegens* Pf-5 strains were inoculated into 50 mL LB media supplemented with tetracycline (50 μ g/mL) from glycerol stock and grown at 30 °C overnight. Cell pellets and liquid media was separated by centrifugation (6,000 rpm, 30 min). The supernatant was acidified to pH=2–3 with 6 M HCl and exacted with EtOAc (50 mL, 3×). The organic layers were combined, washed with brine (50 mL), dried with anhydrous Na₂SO₄, and concentrated under vacuum. The concentrated residue was reconstituted in 2 mL MeOH, 10 μ L of which was injected for HPLC analysis.

Large scale purification of the intermediate 2

P. protegens Pf-5 Δ*pltD* with empty vector pME6010 was inoculated into 5 mL LB media with tetracycline from glycerol stock and grown at 30 °C for 10 h. The seed culture was then added to 1 L LB media supplemented with tetracycline at 30 °C for an addition of 15 h. Cells were removed by centrifugation at 6,000 rpm for 30 min. The supernatant was acidified to pH=2–3 with 6 M HCl. The metabolites were extracted from liquid media with EtOAc (500 mL, 3×). The organic layers were combined, washed with brine (500 mL), dried over anhydrous Na₂SO₄ and concentrated under vacuum. The crude extracts were first purified by silica flash chromatography (DCM to 3:1 DCM/MeOH). All fractions containing the target molecule were pooled, and then purified by preparative HPLC carried out on Luna 5 μm C8(2) 100 Å LC column (250×10 mm) using Agilent 1260 Infinity HPLC system. Water (solvent A) and MeCN (solvent B) with 0.1 % TFA were used as the mobile phase. A flow rate of 2 mL·min⁻¹ was used with the following gradient: 0-5 min: 5% B, 5-30 min: linear gradient to 58% B, 30-36 min: 58% B, 36-38 min: linear gradient to 100% B, 38-43 min: 100% B, 43-44 min: linear gradient to 5% B. Intermediate 2 was isolated as yellow solid. ¹H NMR (500 MHz, CDCl₃) δ 14.41 (s, 1H), 7.34 (d, J = 2.5 Hz, 1H), 4.45 (tt, J = 6.0, 3.8 Hz, 1H), 3.02 (dd, J = 17.5, 3.8 Hz, 1H), 2.94 (dd, J = 16.8, 3.5 Hz, 1H), 2.86 (dddd, J = 21.4, 16.8, 6.0,

1.7 Hz, 2H). 13 C NMR (126 MHz, CDCl₃) δ 202.0, 195.0, 177.9, 125.2, 121.7, 120.7, 114.5, 110.7, 63.2, 47.6, 44.2.

HRMS (ESI) *m/z* calculated for C₁₁H₈Cl₂NO₄ ([M-H]⁻) 287.9836, found 287.9833.

Bioactivity assay

The bioactivities of 1 and 2 were tested in a 96-well plate assay as reported previously.⁴ Briefly, fresh-cultured cells of *Erwinia amylovora* strain LA621 were inoculated in nutrient broth supplemented with 1% v/v glycerol to an OD_{600} 0.01. 1 and 2 were prepared in MeOH and added to the bacterial cultures at different final concentrations up to 400 μ M. The cultures were aliquoted into a 96-well plate which was incubated at 28 °C with a shaking at 350 rpm. The bacterial cultures were amended with or without MeOH and used as controls. The bacterial growth was recorded at 24 h by measuring OD_{600} of the cultures using a plate reader (SpectraMax M2, Molecular Devices). The experiment was performed in quadruplicate and repeated three times independently.

Time-course experiments to monitor PltD activity

The time-course experiments for PltD kinetics were performed in a total volume of 600 μ L containing 0.05–1 mM intermediate **2**, 10 μ M PltD enzyme, and 400 mM potassium phosphate buffer (pH=7.5). Prior to the addition of PltD or mutants, the reaction mixture was incubated at 30 °C for 5 min. At 0, 2, 5, 10, 30, 120, 240 min, 70 μ L of enzyme assays were withdrawn, quenched by the addition of 30 μ L MeOH and analyzed by HPLC. The time-course experiments were conducted in triplicate. Product formation was analyzed against the standard curve of **1** and the initial velocity was calculated. The resulting curve was fit using Origin software to extract K_M and k_{cat} . Time-course experiments of PltD mutants were conducted following similar protocol to wild type, except that 0.2 mM substrate was used in the assay.

SUPPLEMENTARY TABLES

Table S1: Peptide sequences for PltB expression constructs

PltB ^{module1}	MDARAPMDFEPIAIIGSGCRFAKGASTPEAFWELLRAGTDFV
(KS-AT-CP)DEBS2 ^{recognition}	GPVPAERWDTAAIYDESAAETGTTYSKVGAFLEHIDRFDAH
, in the second	YFGISASEAKEMDPQQRLLLEVACESVARAGLTREQLKGSRT
	AVYVGMLGMDYLALHSREAGIEQINPYYAAGKEFSFAAGRI
	AYHLGVHGPAMTVTTACSSSLVAMHLACRALQAGEADMAL
	AGGVNLMLAPDLTIYMSQIRAISPSGRCRVFDAAADGIVRGE
	GCGVTVLKRLADALRDGDPIQAVIRGSAINQDGASAGQTVP
	NANAQAAVISQALKVAGLSVDDIDYVEAHGTGTPLGDPIELS
	SLDSAFQGRERPLWVGSVKANMGHLDAAAGMASVIKTMM
	VLKHAEVPAQLHLAQLNPLVDWKRSRLAVPTAIESLPDRPRL
	AGISGFGLSGTNVHMILEDASVYRQAQPQQERSAQGRPWVL
	PVSARSAQAVVEQARAYAVHLPQQDDGQLQAFVASAIHRR
	DHFPYRSAVVGANAGQLKSQLEQLPAPTLACTTDEEDRRGP
	VLVFTGQGAQWVGMGRDLLEREPAFLAMIRRCDQALAQWA
	SWSVEAELRSDASGSRLHLTEFAQPCIFAIQVAISECLRQWGV
	IPAAVVGHSMGEVAAAYCAGALDLESAVRVIHHRAQAMKD
	TLGQGRMLVVGLPAPTLQSRLANNPQLELSVVNSRNSCVVS
	GSPQAVQALDQQLRDEGIFTYLMPAEYAFHSCQMDECLTQI
	RAGLEDLPVVAAHTPWISTSAMPEEPILADADYWARNARGI
	VRFDRAIEQLIEQGHRLFVEIGPHTVLAASINQALADKGTQGL
	VCGALHKQGDAALELASIVARLYEWGAGPDWQAFQPREAA
	LELPAYPWQQERFWFAPAPRPQPAGLVSQLRAQVLVYDAQG
	NLCAQANDVALSVPQLAQVAVPAPAKVSAAAQPVGDVRAQ
	IGALLTQIIGVACADPDPDRGFFELGLSSISLVEFKRMLERQFA
	LKLSATVGFDYPTINRLGQYLEGLLSREPASTPVTVDAGFAA
	SPAVDIGDRLDELEKALEALSAEDGHDDVGQRLESLLRR
	WNSRRADAPSTSAISEDASDDELFSMLDQRFGGGEDL
PltB ^{module2}	MSGDNGMTEEKLRRYLKRTVTELDSVTARLREVEHRAG
DEBS3 ^{recognition} (KS-AT-CP)	ATDAAGSVAVVAMACRFPQADSPEALWKLMLEQTDTVGPV
	PPSRLAGAKPEETFPRFASLIQRPEGFDEAFFRISPKEARSMDP
	QQRLLLMVAWEALERAGIPQEKLLEQRVGVFVGANSHDYET
	RVLGSAQGVDAHYGTGSSFSAICGRLSHFLGVRGPSLTVDTA
	CSSSLTAIHLACNSLRAAECDIAIVGGVNVIASASIFQSMGQA
	GALAPDGISKAFDDSADGYGRGEGCGVVILKRQAQAERERD
	PIVATILGSAVNHDGACAGLTVPNGPAQEALISEALANAGVH
	PGQVSYVEAHGTGTVLGDPIELNALHNAYRQASPDSPPLTVA
	SVKANIGHLEAAAGIASLIKACLVVEHGRIAPQAHLQRANTR
	VDWAAMNLKLAHQAMDWPGRPESRVAGVSAFGFTGTNVH
	VLLKGYTAPATAPLPPATAPVALCLSAATPAALAELAQRYVS
	FLGATEHCPQTICYNALMRRTAFKERLVVHGQDCRELAQAL
	QAWLAGSPIANDRKPAAGEPWATLAEAFGRGAQSPGPERLP
	DGCQAIGLPTYPWQLNDYWIDAGQPATAVQPARAASGHPCL
	QGLVRPAGQLWYWSGALAPQAGHYDPLGEQGYRVKTHLLL
	DAVLQAVRETPRGVQQIRDLQIAQLRLRGEQHLTSHLSIHLT
	QAPDACFELALQGAGDERRQVCMSGTLVDCAAQLQEETLC
	GVSMLDEPSPPAPDVGLCPWSGCAATGGQRALYRFAHSLTA
	AERQTQLLASVVELFEGAHAAALVGFSGLQVWADLPAQVW

IVLAGHDADKPDSLQVVDARGCQLALFEGPQFGHPGSWYLP DLQTAPLDLPMIARQWQDYPMPGEGARQREGYWMVLAWS TAEVOPLAAAFAAEORPVEVIELHAGOOPLARKLSSALRGA VADPSCLGVIVAGVEAQEADGLGISLVASAALVQAFAGAIAS VGTPAKPVWFALHASDAASPAMAAVQATWQGAAHIFALEH PAWWGGLVTLQGSDRRSYASLCRLLHGQPGHDHFAISGARV EVQYLVEDQADPLQRLEPPALNGTVVLHAVPGSDLETVLTA LGQRGVQRVLLLCEAPGQLHMPERMPEAMAISSLSDLSREN LADTFATLRAQDRIAGFIHLDLDWRTVALKEPEFVVRMQEG VRPLEVLQQVHQLIDDPEAFFLILGSVSSLLGGAGFARSAIAD AYALWVHAQRRRQGLNCQLLHLTQSEQELEQDAAARTAMQ GSGLQPLQRSQIVQAIARVLGGQGQCGLLNVDWQQLKGLYL SVLPWPLLEHLGAADSAADQRLAELIGLPPLQQRRAMQALV CEVVGQVFGVADGLELDVRKGFFDMGMSSVMSLDLRSRLG RALSIDLPSTFGFEYTSIEQVTDYLMGQLLAPETREPVAAPEP VSPASRHQDLHELSRAELIGALEDELRDIANY

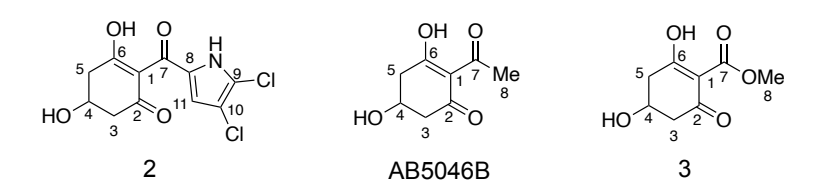


Table S2: ¹H NMR assignments of **2** compared with synthetic AB5046B⁵ and biosynthesized compound **3**.⁶

		δ (ppm)	
Positions	2	AB5046B	3
Н-3	3.02 (dd, J = 17.5, 3.8 Hz,	2.78 (dd, J = 18.0, 5.2 Hz,	2.80 (dd, J = 18.2 Hz, 6.1
	1H)	1H)	Hz, 1 H)
	2.86 (dddd, J = 21.4, 16.8,	2.93 (dd, J = 18.0, 3.2 Hz,	2.93 (dd, J = 18.2 Hz, 4.4
	6.0, 1.7 Hz, 1H).	1H)	Hz, 1 H)
H-4	4.45 (tt, $J = 6.0$, 3.8 Hz,	4.41 (m. 111)	4.27.4.44 (m. 1.11)
	1H)	4.41 (m, 1H)	4.37-4.44 (m, 1 H)
H-5	2.94 (dd, J = 16.8, 3.5 Hz,	2.64 (dd, J = 16.4, 6.4 Hz,	2.64(dd, <i>J</i> =16.4, 6.8 Hz, 1
	1H)	1H)	Н)
	2.86 (dddd, J = 21.4, 16.8,	2.74 (dd, J = 16.4, 1.0 Hz,	2.76(dd, J= 16.4, 3.8 Hz, 1)
	6.0, 1.7 Hz, 1H).	1H)	H)
Others	14.41 (s, 1H, NH)		3.89 (s, 3 H, OCH ₃)
	7.34 (d, J = 2.5 Hz, 1H, H-	2.59 (s, 3H, H-8)	6.87 (br s, 1 H, OH-4)
	11)		14.68 (s, 1 H, OH-6)

Table S3: ¹³C NMR assignments of intermediate **2** compared with synthetic AB5046B⁵ and biosynthesized compound **3**.⁶

	δ value in ppm		
Positions	Compound 2	Synthesized AB5046B	Biosynthesized Compound 3
C-1	110.7	113.3	105.3
C-2	202.0	196.3	191.2
C-3	44.2	47.0	47.2
C-4	63.2	63.4	63.5
C-5	47.6	41.6	39.3
C-6	195.0	193.3	188.7
C-7	177.9	202.3	172.2
Others	125.2 (C-8) 121.7 (C-9) 114.5 (C-10) 120.7 (C-11)	28.4 (C-8)	52.8 (OCH3)

Table S4: Peptide sequences for PltD and homologous proteins

GenBank accession number	Peptide Sequences
AAD24878.1 PltD	MNDVQSGKAPEHYDILLAGNSISVIMLAACLARNKVRVGLLRNRQMPP DLTGEATIPYTSMIFELIADRYGVPEIKNIARTRDIQQKVMPSSGVKKNL GFIYHQRSRAVDLGQALQFNVPSEHGENHLFRPDIDAYLLAAAIGYGAQ LVEIDNSPEVLVEDSGVKVATALGRWVTADFMVDGSQGGQVLARQAG LVSQASTQKTRTLEFSTHMLGVVPFDECVQGDFPGQWHGGTLHHVFD GGWVGVIPFNNHQHSRNPLVSVLVSLREDLCPSMDGDQVLAGLIELYP GLGRHLSGARRVREWVLRQPPRQVYRTALERRCLMFDEGAASNDLLFS RKLSNAAELVLALAHRLIKAAHSGDYRSPALNDFVLTQDSIISLSDRIAL AAYVSFRDPELWNAFARVWLLQSIAATITARKINDAFAKDLDPRVFDEI DQLAEDGFWMPLYRGYKDILNTTLGLCDDVKSAKVSAAHAASSIFAEL ANASFVPPIFDFANPHARVYQLTTLRKLKALWWGLMQVPSEVGRLIFY RSFRKPSLRKES
AFP87522.1 Mpy5	MPAKKTRKATRGRPAAPRETYDVAVLGAHLSGGLLAAILAHRG ARVVLVDTPDDHAGTPGETTVPYTSEVFALLASRFDIPEIATFAHF TDLPDEVRTSSGVKRSLGFLYHERGHEQDPRKSVQFNVPGEHTE WHLYRPTVDAYARRIAATYGAERDPAGAPLRAVSLHDEGVDLT LEGDRELTARYVVDASGPDSPLLAAAGVSGVPSDSPHLPLRSRLL SAHLTGVRPYEQVAAQSRYQNTTDWSLGSFHHVFDGGWIEVVD FANHSASQNRHTSVTVSVCPTKFADLPDDPEAAFRALIARFPSVA GQFATASVVGSWTHAPAWQWRAERTFGRRWLAIDRAAVRAE EVLARDVTVSMELVHATAVGLLRVLRDPDVEQREFERIATYQDR LTEYNDQLQQGLRTASGHFQLLNAYLRVWLLWQILADLALKRA RLECGDGPGQSWDAVEEFDSALWFRTPEGLGRALRHTFDQLAK VRRQDTREVTAAREIFAWLSRERFVPPLYRFADPKATVYKFTAW RRVLMLLWVKTLAPADFQRLLTRDNVTGRRDDAPPT
ABO15847.1 Pyr11	MKAIKSPEHDRRLARAADPAEKYDVAILGGSMAAGLLGAVLSR QGVRVLLVGAADDDSDPAGETTVPYTAEVFLLLAKRFQVPEIAA FGLFTDLPPWVRSESGVKKSLGFLYHHPGRPQDPHECVQFNVPN EHGEWHLYRRGVDRYTRELAAKYGAALAGADVFVSDAWVEED EGRVRVSDGTVYRARFLVDCVGPDSPLLVRNGGDDAEPRLRHTS RVYATQMRGVVPFEALVPPSRQDKVTPWSEGTVHHLFDGGWVQ LVDFGNHKESRNPTTSVTLSVDPERFPDLPEEPDKAFRQVVERFP DLARQFENATPVRPWTVETRYQRTASTTHGERWFGLERTAARN DMFLARDATMAAESVHALASVLIPAVRRDNWSPAPFARVALFQE ALGEFNDRLLHAARTACQDFRLWNAFSRVWLLWQILADLSLKR ARLDAESSGDWSVCEQYELGGIWFQCPRGLRELIDRSLETVDEVR RGGLAAGAAADRIFAELRREPFVPPLYAFGDPGARVYRFTLPKRL QMLFWVKTKAPADFRRLLTVDNVSGVTAASSR
AGC24267.1 PrlM	MTVETPSTPFDVAVLGTHLGCAMLAAILAKQGVRVLLVDAAPG QEEFAGETTVPYTAEVFFTLARRFDIPELAAFGLTSALPSEIRRSSG IKRSLGFLHHSEGRQQVPEQAVQFNVPGEHAEWHLYRPHVDQH AWTIARRYGAVVVPHRPAVADVRVGAGGADVLLADGSLHRARF VVDGSGAGSPLVRRLGAEDAAPKLRSRSRVLATHMYGVRPYEQ CVRQADYVSATDWSMGTISHLFPGGWLQLAHFGNGEDPVNPLT

	CVVI CLDDCDVADI DCDDECAEDEI VDDEDTI ADCEVDAVAADD
	SVVLSLDPGRYADLPGDPEQAFRELVRRFPTLARSFKDAVAARP
	WTAARVWQRTAGPAFGEGWFLFDRTFSRNDLFLSRDVTMTAEM
	VHALAPALVEAARRDDWSTPALRRAALFQERLVDFNDRLLAGA
	RTATTDFRLWNAYSRVWLLWSMLSALSLKSARNRCLARGRWEE
	VERFGDDAFWFRPPDGLPGLLDRALGELAEVEAGTRSASACAGR
	LFTLLRRAPFVPPVYRFADPDARYYHFSTARRLRMLLWSKTVAP
	AEFRTMMTKENLTNVPPPAMH
	MRSTIDPGADHQVAVIGTGVTGAMLGAVLARNGVRVLLLGPDE
	HPRHEPGELTLPCTSFLYELIAARYRVPEIAFLAFADKVREEISGA
	GGVHRTFGFAHHTEGRAHRRYESLQFNVPSEHGESHLYRPDVDA
	WLLALAVRHGAEVRQRVRVEKAIPEDGGVRLVTAAGEEITAAC
	VVDTSGPGSAVAQALGGTVERAGGTTRVLSAHAVGVRPFDEVSP
	HLDGSPPWHEGTLHHVFDGGVLAVSHFGNAGKTLERTALTSVCL
TNM30593.1	TLTGEGTPAGDGGWAEIRSHLERFPSLAAQFAEARPLVTWADEQ
	PEWHATVTAGDRMLLLDRAALGGSPLLGRDLYVSAQLVHTAAA
	DLLGAARDGDFGVGRFRYLQALQHGMAARQRRLTAAVHAAGG
	QFPLWNAMGRVWLLGTMLDALTLKRGLKLLNAGQIEQASAALR
	TRAPETGACHQTLTEYEELLDWTLAECELVRSGEATSRQASDRIF
	QRLRRERIAPPIYGFGEPDDLDYGLSLRRRLRTLRWVRKDAAPAV
	RRLVRSYGVRGGGGGIEDD
	MTRPDPSERYDVALLGGHLATGMLGAVLARQGLRVLVVAAPGD
	RTEVSGETTVPYTSEVFMLLAHRFEVPELAAFGRFPDLPAGLRRG
	SGVKRSLGFLYHRAGAVHDPEESIQFNVPGEHTEWHPFRPDVDR
	YAVRLAEKYGAAATSSDDELVDAWVEPDGNGAPAGRVETSGGH
	VYRARFLVDAAGTDSPLVRRNGGDDAEPRLRHRSAVLTARMHD
TMR02610.1	VTPFEELVDASRYPKASLWSRGTVHHLFEGGWLQLAAFGNHEDS
1 MIKU2010.1	RNRSTSVTLSLDPAALADLPSDPGAAFHTVVDRFPDLKRQFENAV
	PVSWRVAPLVQRTAARTHGEGWFAFERSAARNDLFLARDVTTS
	AELVHSLAAALIPAFADGDLSPGRFERAARFQHELAAFHDSWIDG
	ARTACADFALLNAFSRVWLLWQILADLSLKRARLDCKVAAARG
	RADWSPVERFELGGLWFQAPAGLRETIAFTMDRLAQVRAGLIDP
	RSAADDVFGRLRTADFVPPLYAFGDPGARIYRFTLPKRLQMLWW
	VKTKAPSDFRRLLTRDNVTSVSTRSSR
	MAVADRAIRYDVAVLGAHLGGCLLAAVLARHGLRVLLVDAPSD
	SDEFAGETTVPYTAEVFFTMARRFGMPELAGFGLTSALPSEVRRS
	SGVKRSLGFLYHREGHEHDPALAVQFNVPGEHAEWHPYRPHVD
	RYAYLLALRYGAVAPPQRPVLADVRVGEEEVNVLLRDGSLHHA
MBB6471016.1	RFVVDGAGAGSPLSDRLGAEDEIPRLRLRSRLLATHMQGVTPFEE
	CVRLEDYGQATPWSKGTLTHVFPGAWVQVAHFDNGEDPVNPLA
	SVVASVDPVRYADLPADPEDAFRELIGRFPSLARSFSNAIACRPW
	TSARRWQRTAGTTAGERWFLWDRTAARNDFLLSRDVTMTAEM
	VHALAPALIEAAAGDDWTGHVRPVAVFQERLVDFHDRLLTAAR
	AATEDFRLWNAYSRVWLLWSMLSALSLKSARNDCLARGRWDG
	VRGHHGHAFWFAPPKGLNRLLSQVFEEFGEVEAGTRSAGAAAG
	RVFALLREAPFVPPVYRFADPKARYYHFSAARRLRMMLWSKTT
	APVEFRRMMTKENLTSVQPDALH
	I TO THE THE TELL OF YEAR IN THE TELL OF T

AR AFG
\ ⊢ (→
HA
RV
VIA
RF
DM
IDL
DE
RA
RV
RLK
.GD
ELS
DL
EIR
/ER
LAT
DΑ
DL
.QD
AA
.GR
TL
LAR
TF
ЗЕН
ĠΑ
SR
VD
IA
EV
LID
ME
RA
RI
/TT
ONDERS - VEORIT - VEO

SUPPLEMENTARY FIGURES

Figure S1: Scheme for the one-pot enzymatic synthesis of dichloropyrrolyl-*S*-PltL starting from dichloropyrrolyl acyl-*S*-pantetheines using CoaA, CoaD, CoaE and Sfp enzymes.

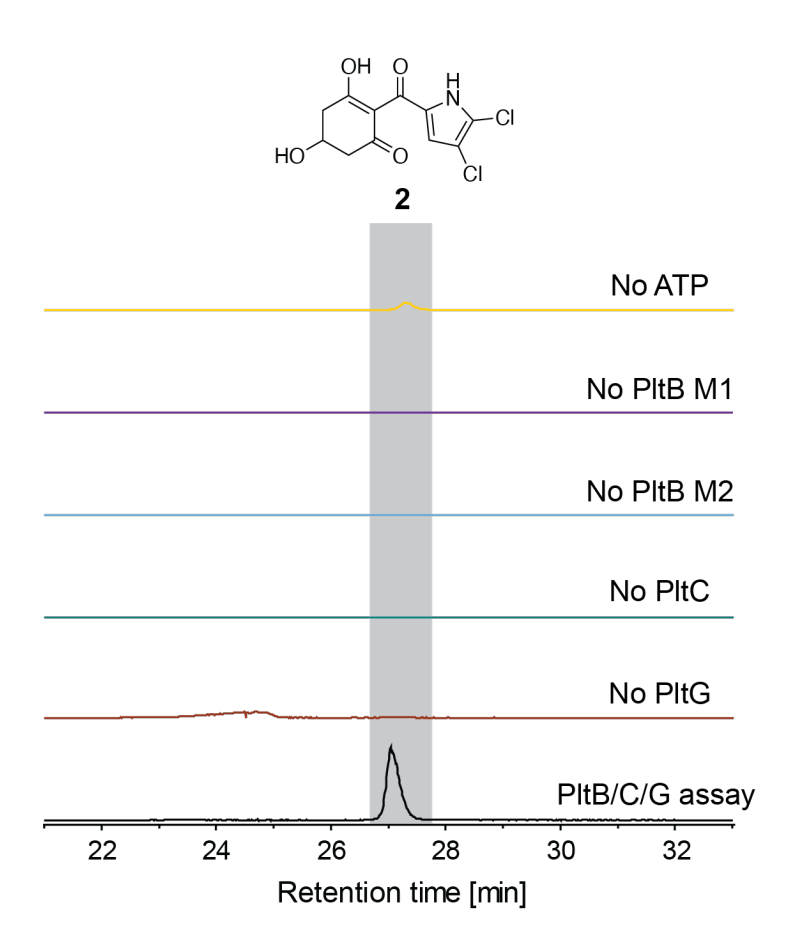


Figure S2: Intermediate **2**, as denoted by extracted ion chromatograms (EICs) corresponding to m/z 287.98 Da, is not produced in the absence of ATP, PKS modules or PltG. Trace amount of **2** was produced without the addition of ATP which might result from ATP bond to purified proteins.

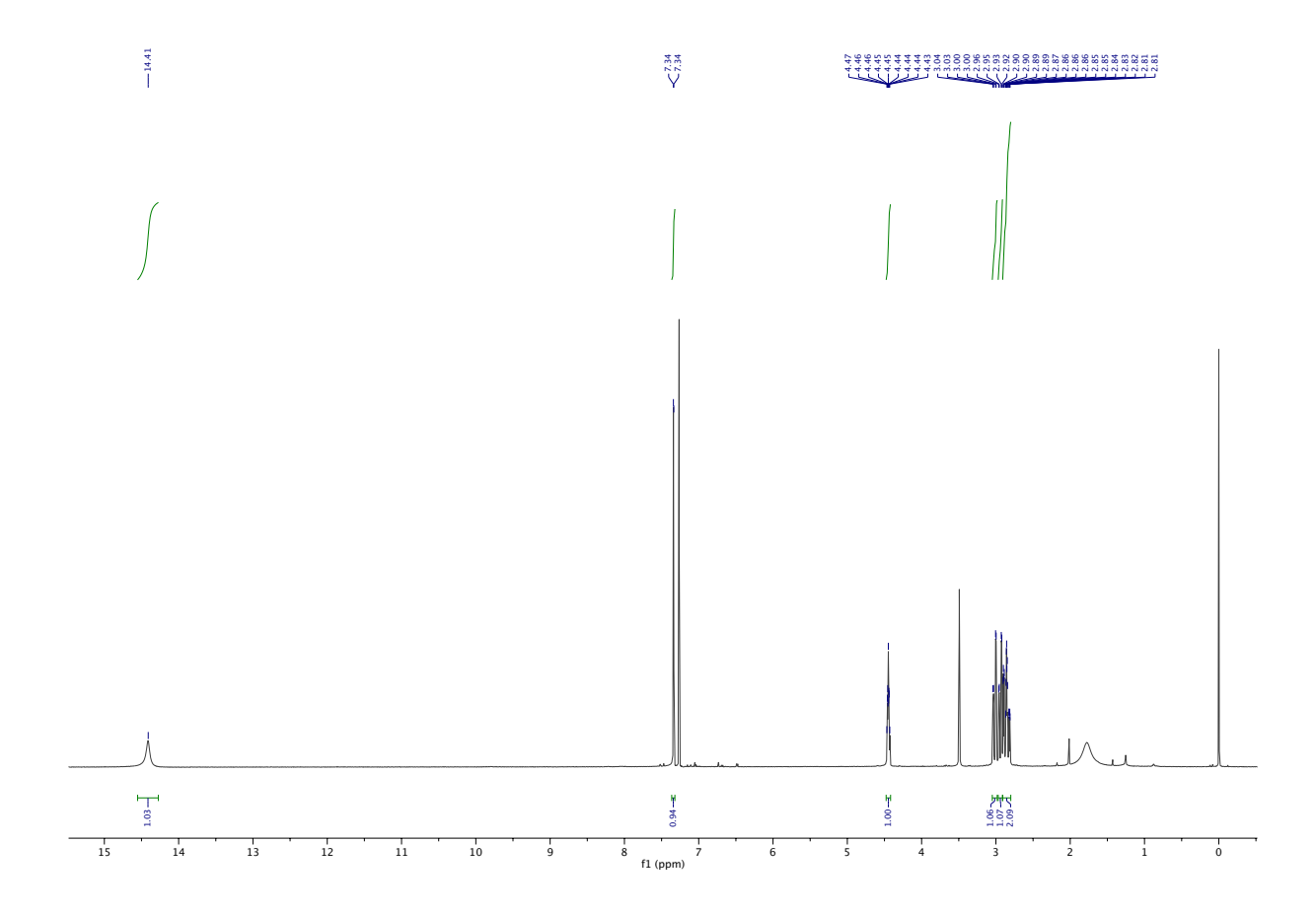


Figure S3: ¹H NMR spectrum (500 MHz, CDCl₃) of 2

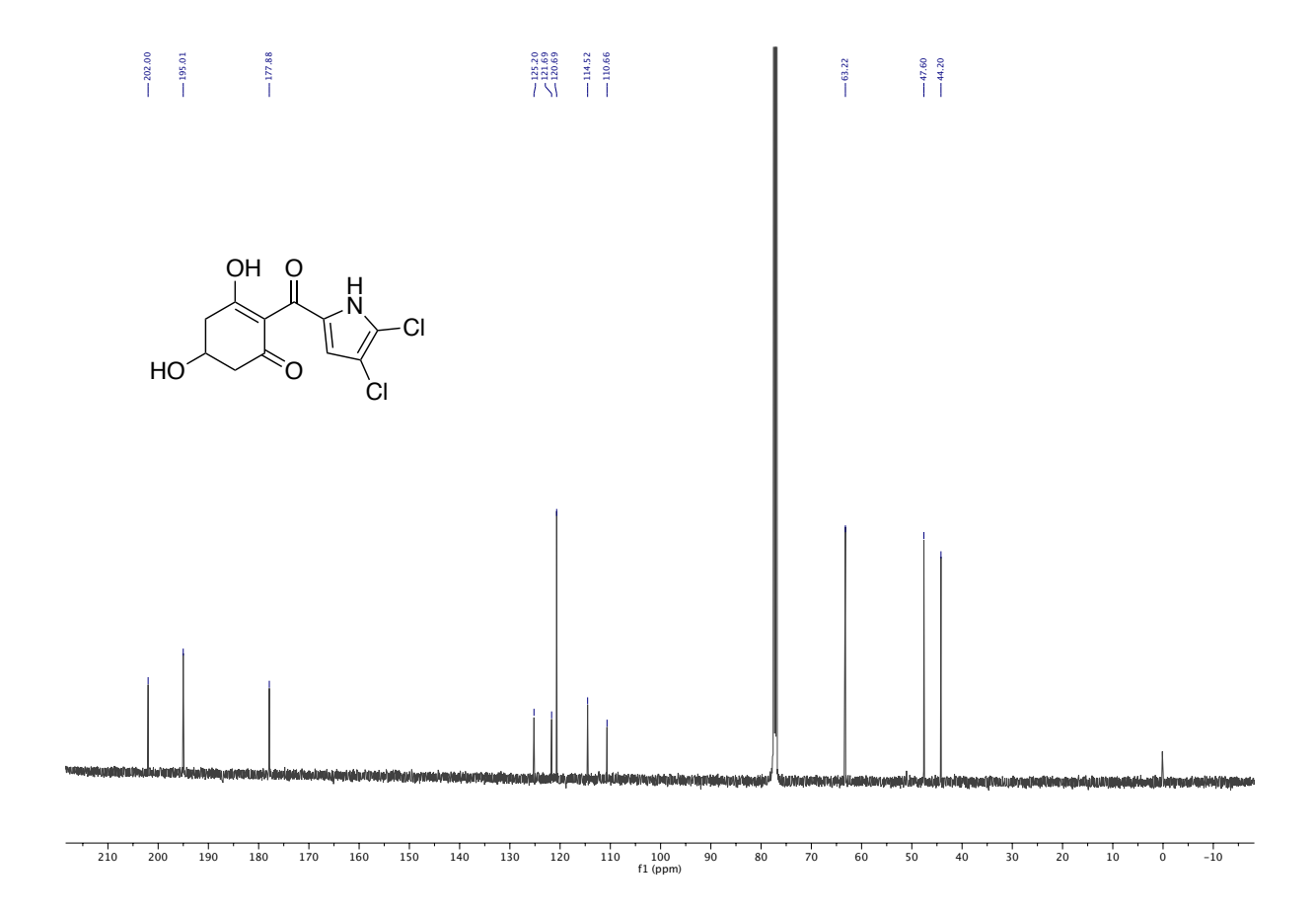


Figure S4: 13 C NMR spectrum (126 MHz, CDCl₃) of 2

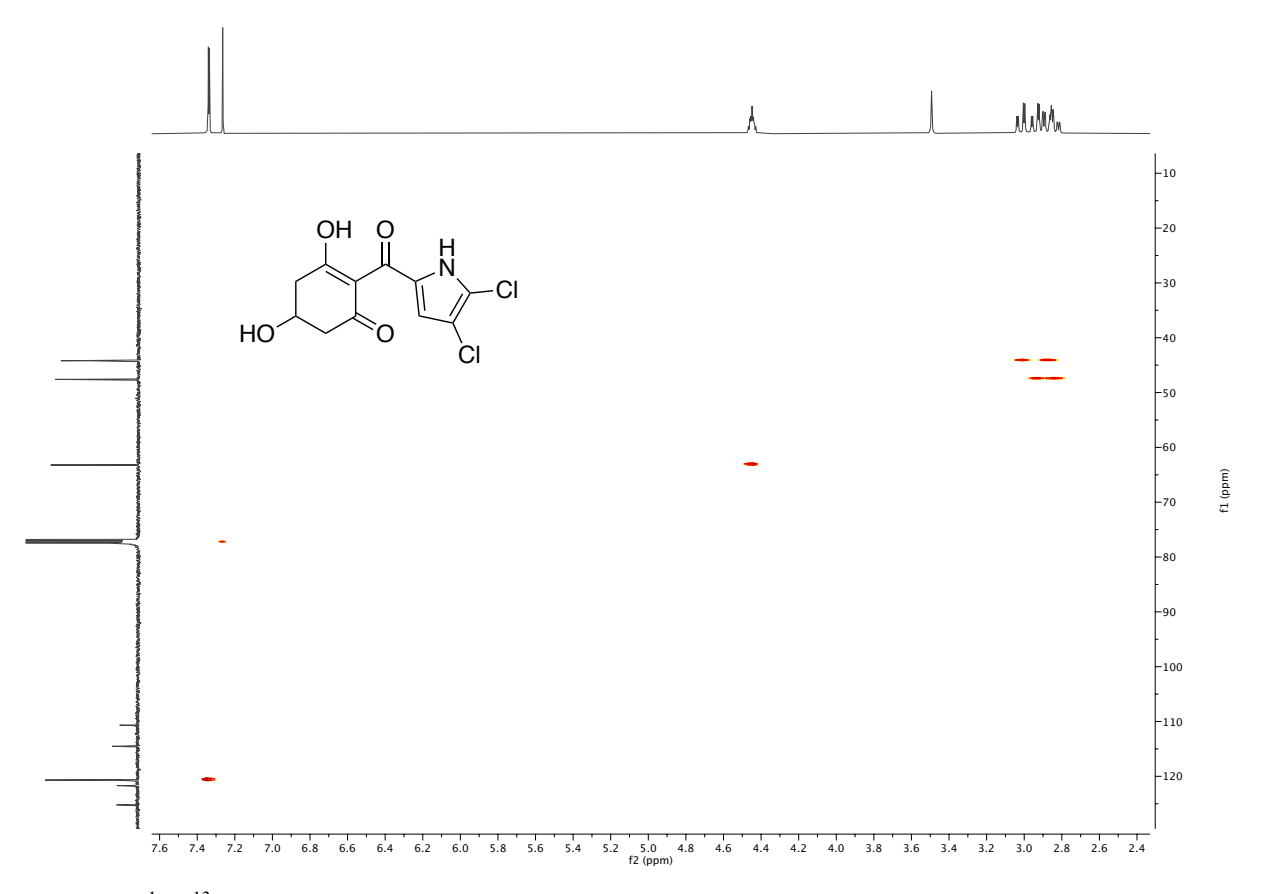


Figure S5: ¹H - ¹³C HSQC spectrum compound **2** in CDCl₃.

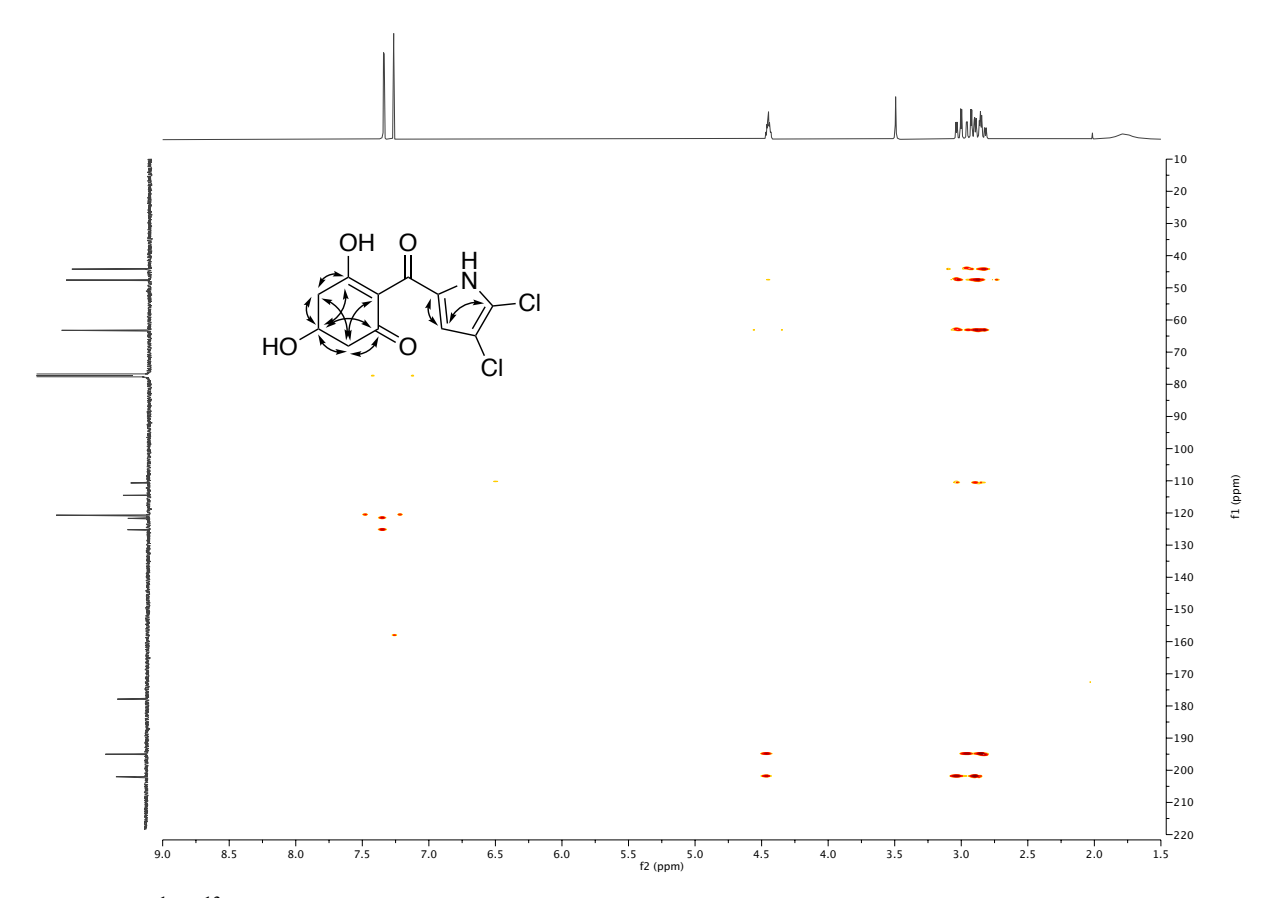


Figure S6: ¹H - ¹³C HMBC spectrum compound **2** in CDCl₃.

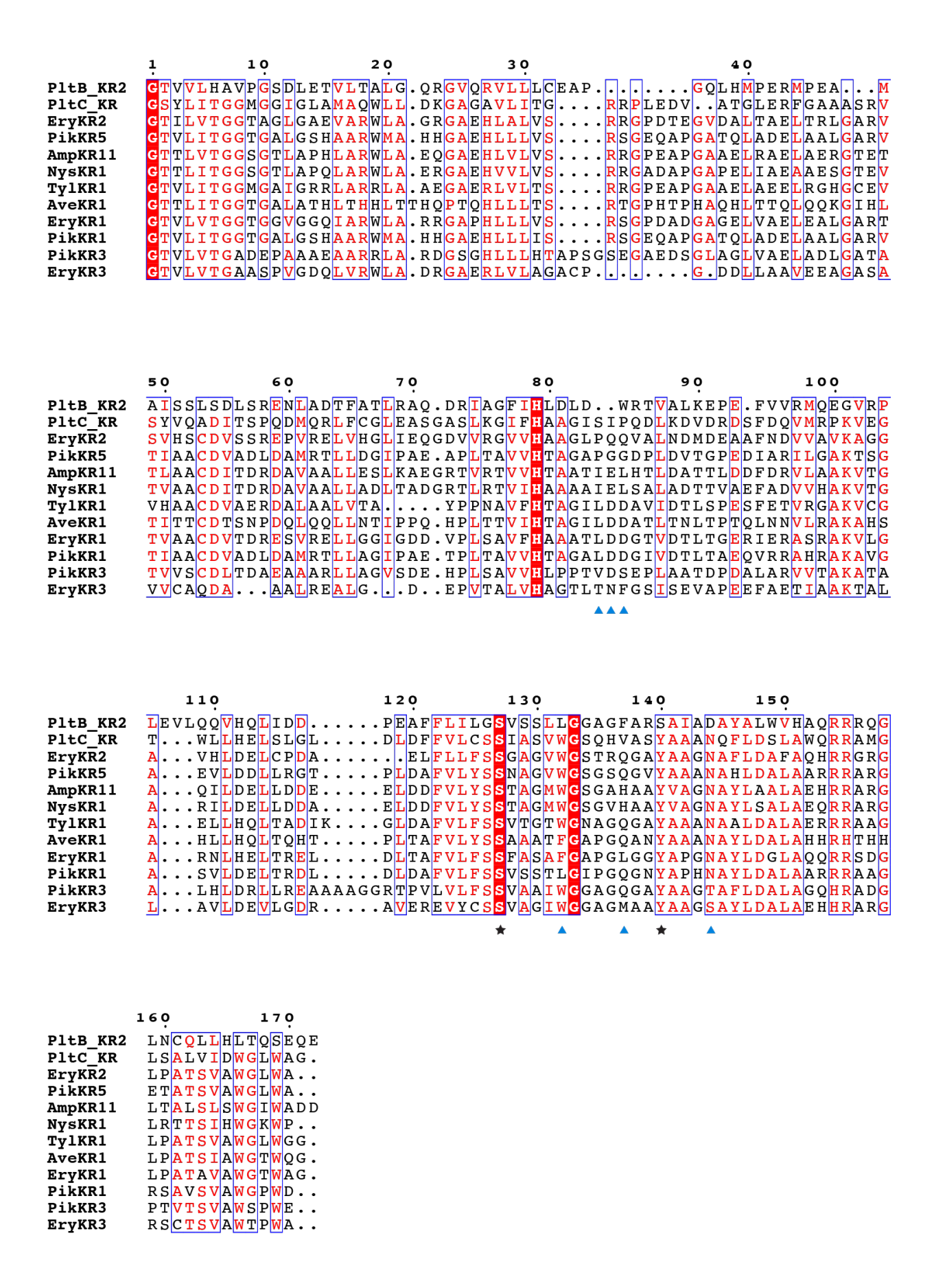
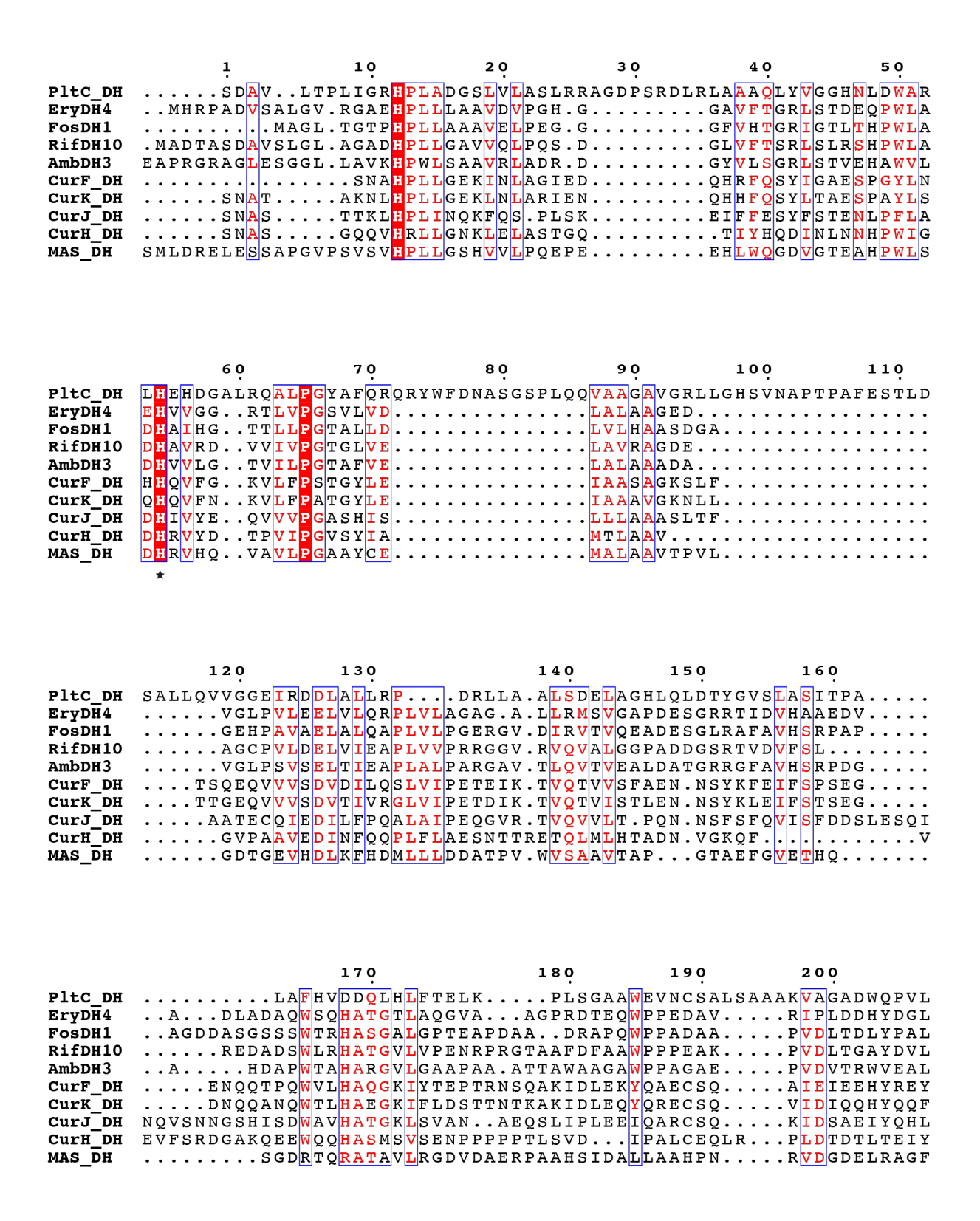


Figure S7: Sequence alignment of PltB_KR2 and PltC_KR with other reported KR domains from erythromycin, pikromycin, amphotericin, avermectin, nystatin, tylosin assembly lines using Clustal Omega. Residues with more than 70% similarity were colored in red and framed in blue. The figure was generated by ESPript 3.0. Catalytic serine and tyrosine residues are indicated by black asterisks and other key residues between different types of KR domains are indicated by blue triangles, which include the LDD motif of B-type KRs, the conserved tryptophan of A-type KRs, the conserved histidine of A2-type KRs, and the conserved asparagine replaced by a smaller residue in C2-type KRs. The absence of catalytic tyrosine in PltB_KR2 indicated the KR domain in the second module of PltB is non-functional. In addition, because of the presence of conserved tryptophan and absence of LDD motif, the KR domain of PltC is predicted to be an A-type KR which produces a hydroxyl group of 'S' stereochemistry.



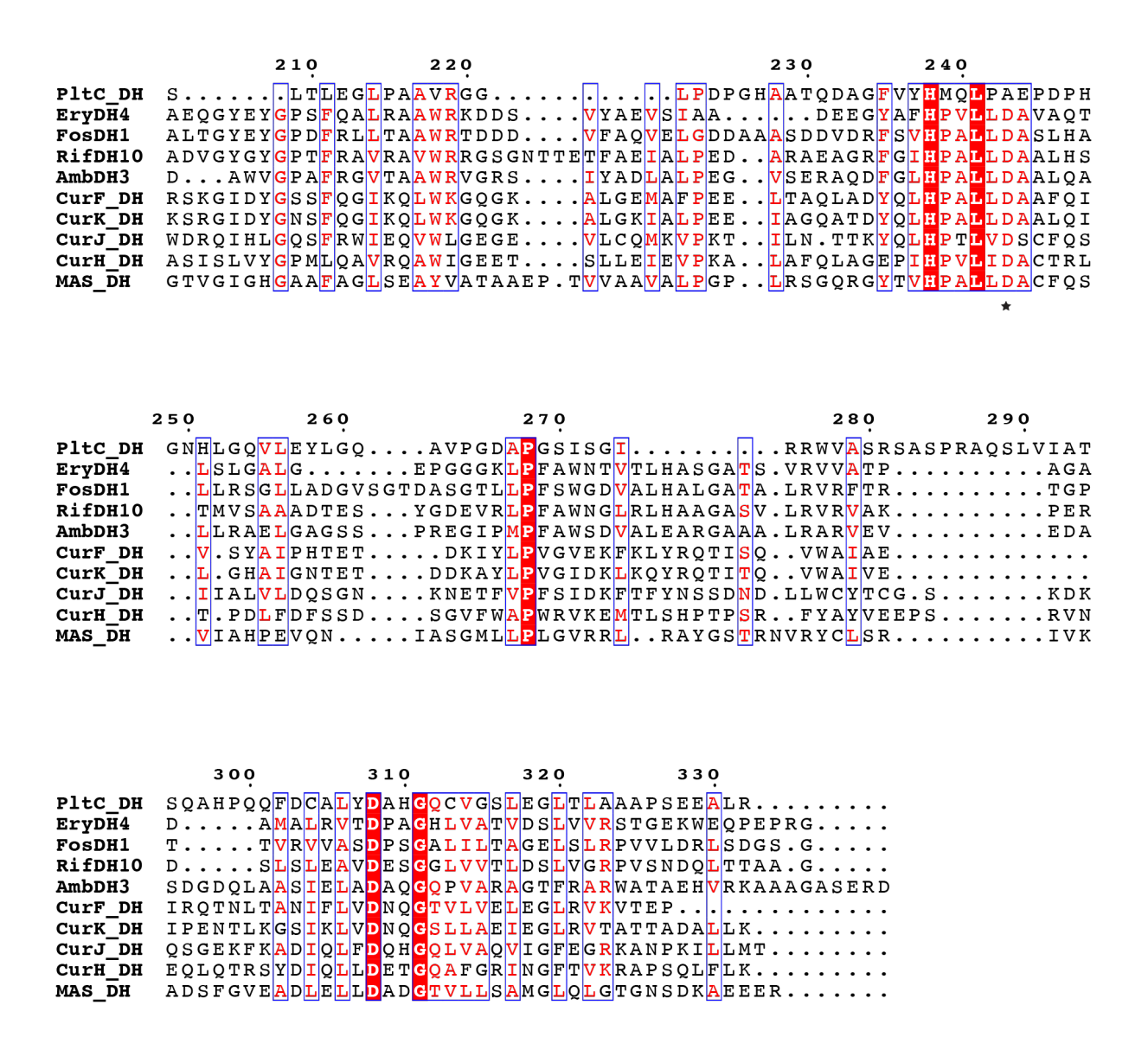


Figure S8: Sequence alignment of and PltC_DH with other reported DH domains¹⁴⁻¹⁹ using Clustal Omega. Residues with more than 70% similarity were colored in red and framed in blue. The figure was generated by ESPript 3.0. Catalytic histidine and aspartate residues are indicated by black asterisks. Limited sequence similarity identified as well as the absence of catalytic aspartate indicates that the DH domain of PltD is non-functional.

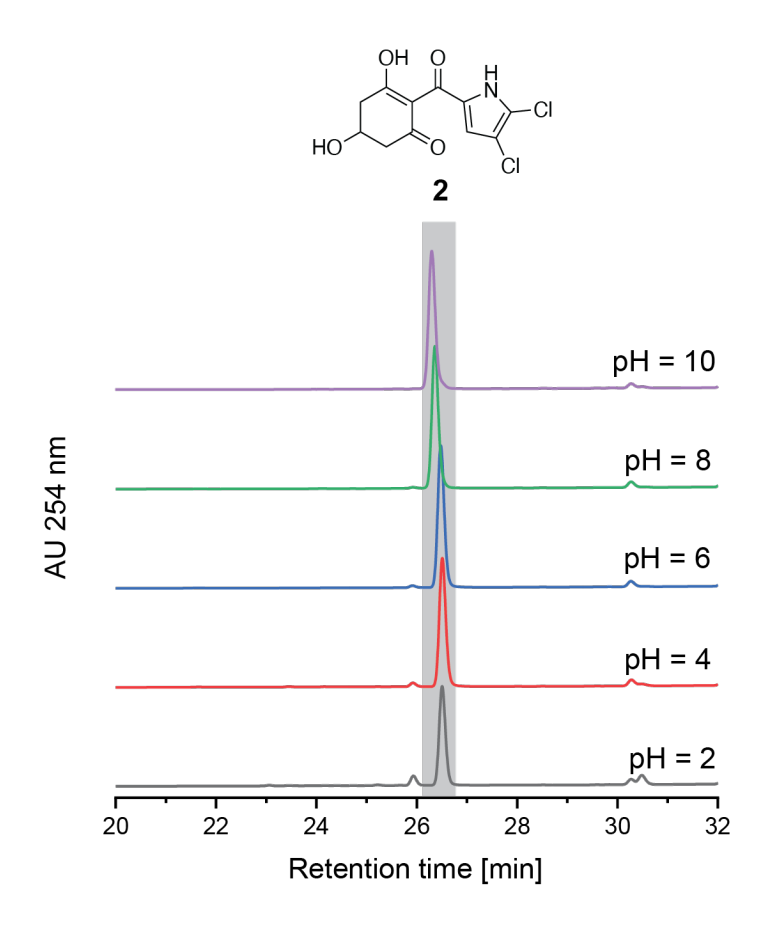


Figure S9: Stability of **2** at pH ranging from 2 to 10. **2** (0.2 mM) was incubated with 400 mM potassium phosphate buffer (pH=2–10) in a total volume of 100 μ L at 30 °C for 22 h. Trace amount degradation was observed at pH=2.

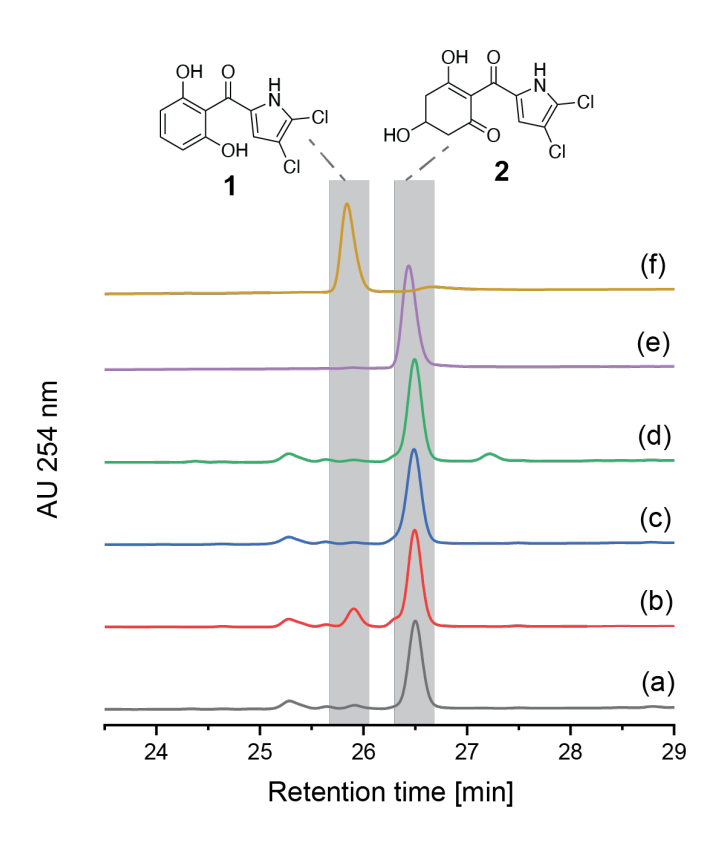


Figure S10: Comparative HPLC analysis for the production of **1** in PltB/C/G assays with the addition of protein extracts from *Pseudomonas* strains: (a) boiled *P. protegens* Pf-5 protein extract; (b) *P. protegens* Pf-5 protein extract; (c) *P. aeruginosa* PAO1 protein extract; (d) *P. aeruginosa* PA14 protein extract, (e) standard of **2**, and (f) standard of **1**. Production of **1** was only observed when the protein extract from *P. protegens* Pf-5 was added to PltB/C/G assay, but not with the other two *P. aeruginosa* strains.

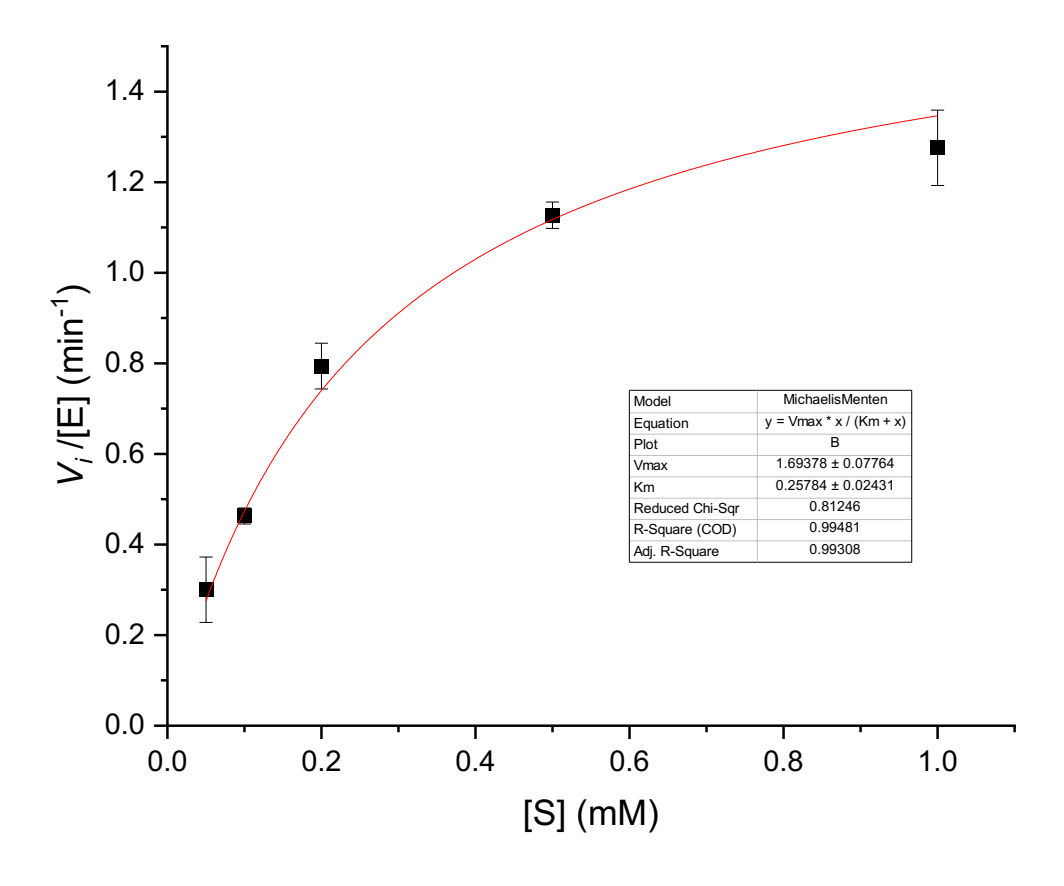


Figure S11: Michaels-Menten kinetics curve for PltD.



Figure S12: Toxicity of the wild type *P. protegens* Pf-5 strain (LK099) and the $\Delta pltD$ mutant strain (LK283) against the target bacterium *Erwinia amylovora*. Fresh-cultured cells (OD₆₀₀ = 1.0) of LK099 and LK283 strains were inoculated in nutrient agar amended with 1% glycerol (NAGly). The plates were incubated at 28 °C for 24 h. The bacterial cells were then killed by chloroform treatment. The plates were overlayed with *E. amylovora* (LA621) cells in warm NAGly at a OD₆₀₀ of 0.01 and incubated for 24 h before the results were recorded. The experiment was repeated two times with similar results. Note that *P. protegens* produces numerous antibiotics in addition to 1; the bioactivity of the LK283 strain is likely attributed to those antibiotics other than 1.

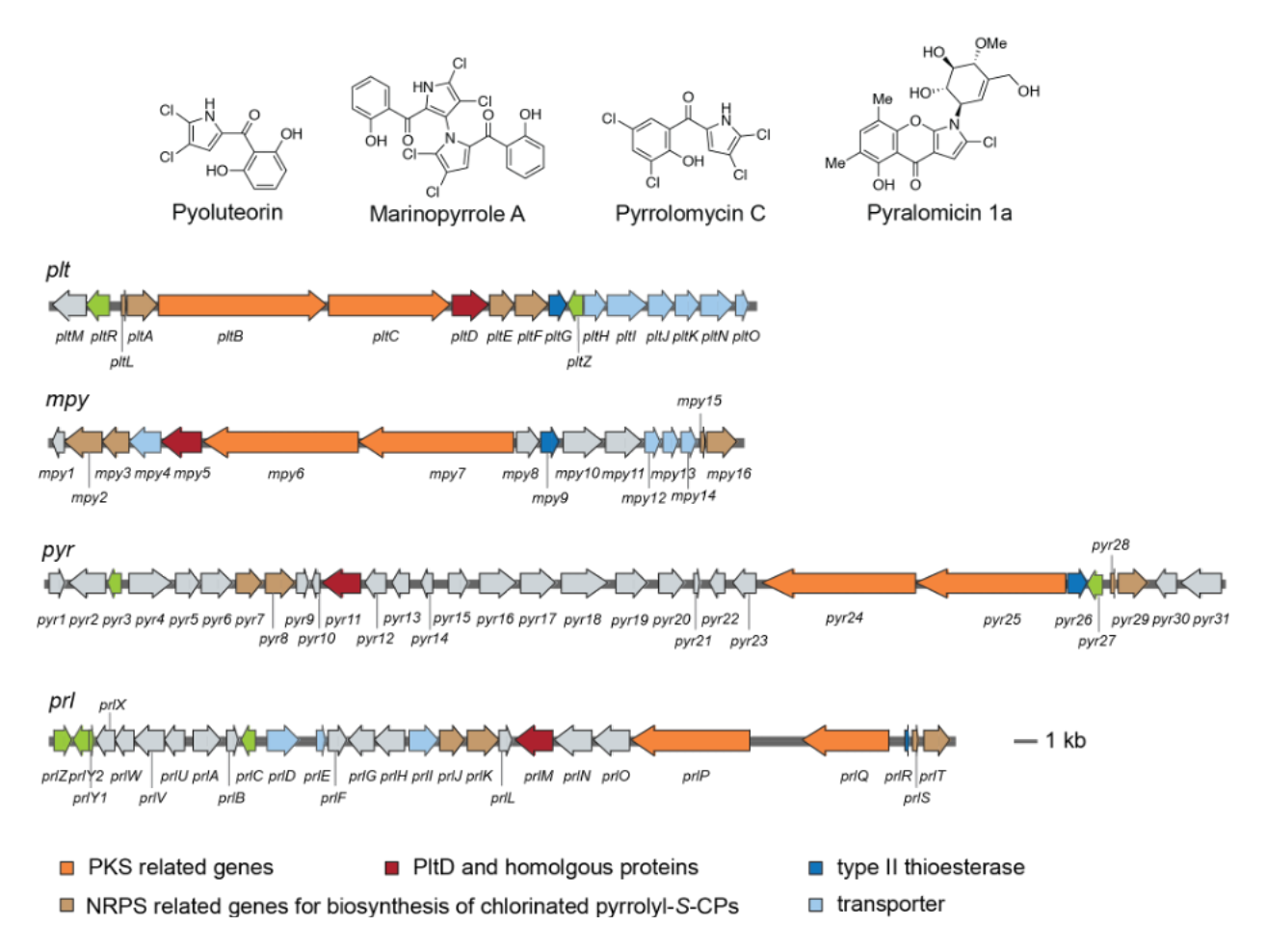


Figure S13: Gene organization of the pyoluteorin²⁰ (plt) gene cluster compared with biosynthetic gene clusters for marinopyrroles (mpy),²¹ pyrrolomycins (pyr),²² and pyralomicins (prl).²³ Genes encoding type I PKS and PltD homologous proteins are present in all gene clusters.

Figure S14: Proposed mechanism for the dehydrative aromatization reaction catalyzed by PltD. A catalytic base would extract a proton from the dihydrophloroglucinol substrate to set up the formation of the dehydrated ketone which rapidly tautomerizes to the aromatic enol.

Figure S15: Mono- and dichlorination of phloroglucinol catalyzed by PltM.²⁴ Halogenation of aromatic substrates by flavin-dependent halogenases can be thought to proceed as two half reactions. In the first half reaction, the halogenase oxidizes the chloride to a chlorinium ion (which is biologically accessible as hypochlorous acid or as a chloroamine bound to the catalytic lysine residue side chain). The first half reaction requires the participation of a flavin reductase (abbreviated as Fl. Red in the figure above; in ref. 24, the *E. coli* flavin reductase SsuE was employed for *in vitro* activity assays). The flavin reductase uses NAD(P)H to reduce FAD to FADH₂, with FADH₂ then available to the halogenase *in situ* as a substrate. The flavin cofactor serves to deliver four electrons (two electrons derived from NAD(P)H and two electrons derived from chloride) to molecular oxygen. The second half reaction involves a redox-neutral electrophilic aromatic substitution reaction using the chlorinium ion.

PltD	4	VQSGKAPEHYDILLA GNSISV IMLAACLARNKVRVGLLRNRQMPPDLTGEATIPYTSMIF	63
PltM	15	VPRGSHMNQYDVIII GSGIAG ALTGAVLAKSGLNVLILDSAQHPRFSVGEAATPESGFLL	74
PltD	64	ELIADRYGVPEIKNIARTRDIQQKVMPSS-GV ${f K}$ KNLGFIYHQRSRAVDLGQALQFNVPRLLSKRFDIPEIAYLSHPDKIIQHVGSSACGI ${f K}$ LGFSFAWHQENAPSSPDHLVAPPYKVP	120
PltM	75		134
PltD	121	SEHGENHLFRPDIDAYLLAAAIGYGAQLVEIDNSPEVLVEDSGVKVATALGRWVTADFMVEAHLFRQDIDYFALMIALKHGAESRQNIKIESISLNDDGVEVALSNAAPVKAAFII	180
PltM	135		190
PltD	181	DGSQGGQVLARQAGLVSQASTQKTRTLEFSTHMLGVVPFDECVQGDFPGQWHGGTL	236
PltM	191	DAAAQGSPLSRQLGLRTTEGL-ATDTCSFFTHMLNVKSYEDALAPLSRTRSPIELFKSTL	249
PltD	237	HHVFDGG WVGVI PFNNHQHSRNPLVSVLVSLREDLCPSMDGDQV-LAGLIELYPGLGRHL	295
PltM	250	HHIFEEG WLWVI PFNNHPQGTNQLCSIGFQFNNAKYRPTEAPEIEFRKLLKKYPAIGEHF	309
PltD	296	SGARRVREWVLRQPPRQVYRTALERRCLMFDEGAASNDLLFSRKLSNAAELVLALAH	352
PltM	310	KDAVNAREWIYAPRINYRSVQNVGDRFCLL-PQATGFIDPLFSRGLITTFESILRLAP	366
PltD	353	RLIKAAHSGDYRSPALNDFVLTQDSIISLSDRIALAAYVSFRDPELWNAFARVWLLQSIA	412
PltM	367	KVLDAARSNRWQREQFIEVERHCLNAVATNDQLVSCSYEAFSDFHLWNVWHRVWLSGSNL	426
PltD PltM	413 427	ATITARKINDAFAKDLDPRVFD 434 GSAFLQKLLHDLEHSGDARQFD 448	

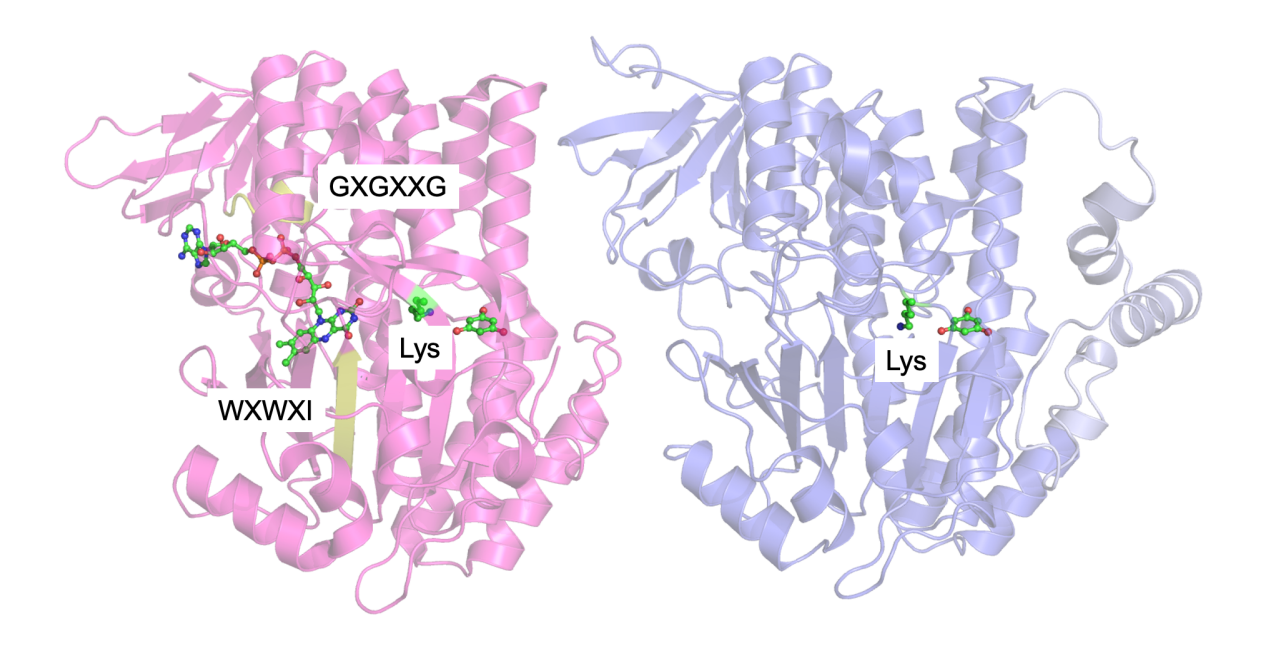


Figure S16: Sequence and structural alignment between PltD and PltM. PltD does not possess the GXGXXG and the WXWXI (highlighted in yellow) sequence motifs characteristic of flavin-dependent halogenases. In the structure of PltM (bottom left), position of these two sequence motifs is highlighted in yellow. The flavin cofactor, the phloroglucinol substrate, and the lysine side chain critical for halogenation activity are shown in stick-ball representation with carbon atoms colored green. The lysine residues are highlighted in yellow in the sequence alignment.

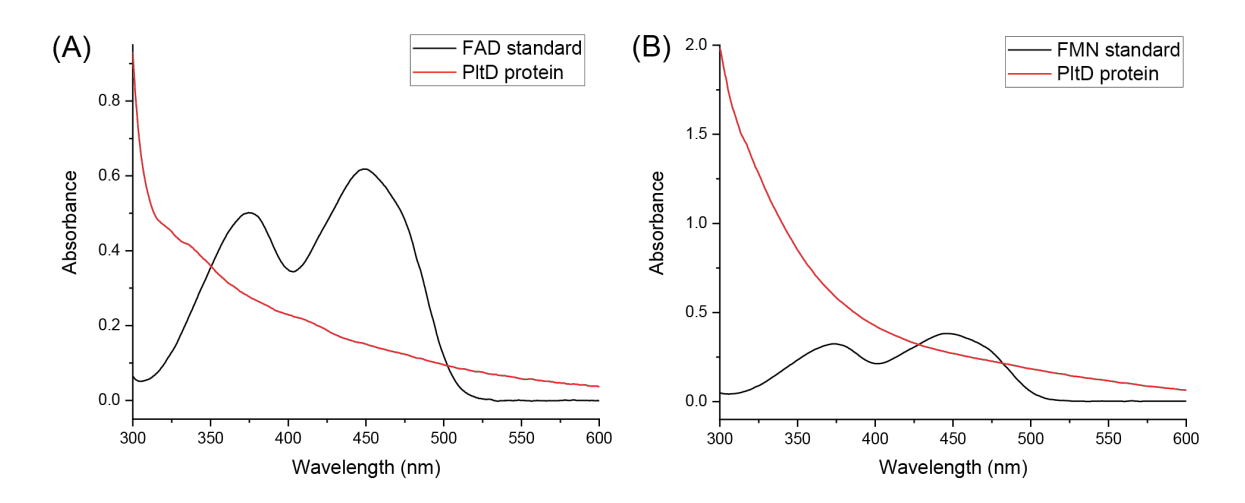


Figure S17: UV-Vis absorbance spectra of PltD compared with (**A**) flavin-adenine dinucleotide (FAD) and (**B**) flavin mononucleotide (FMN) standards. Recombinantly expressed and purified PltD was incubated with 10-fold molar excess of FAD or FMN overnight, followed by the removal of unbound FAD or FMN using desalting PD-10 columns. Spectra were recorded in 20 mM Tris-HCl (pH 8.0), 500 mM NaCl, 10% glycerol buffer. No absorbance peaks observed at 375 and 450 nm for the PltD protein sample indicated that PltD did not bind a flavin cofactor.

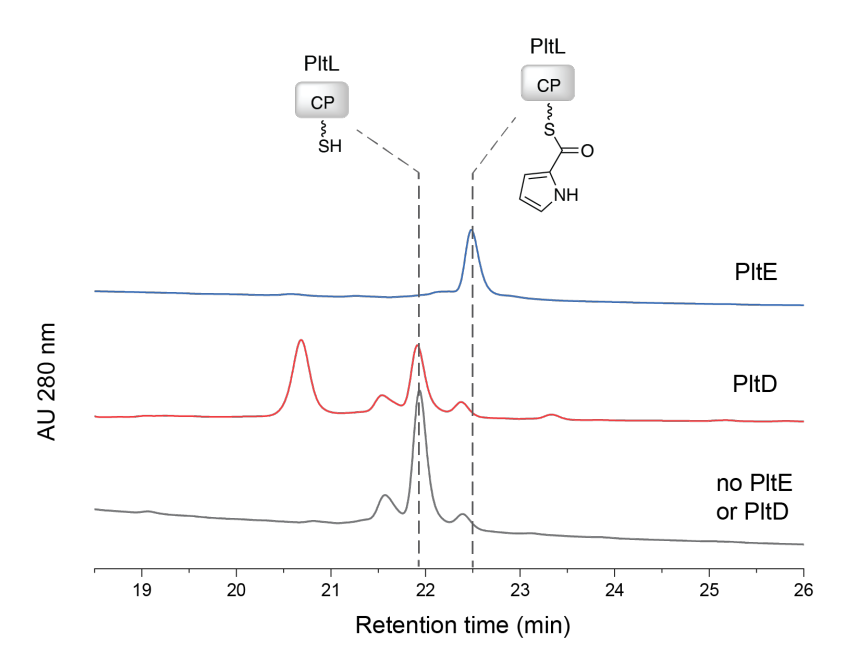


Figure S18: Lack of proline oxidation activity for PltD. In pyoluteorin biosynthesis, the amino acid L-proline is thioesterified to the phosphopantetheinyl thiol of the carrier protein (CP) PltL by the adenyltransferase PltF, followed by the oxidation of the prolyl-*S*-PltL to pyrrolyl-*S*-PltL by PltE.²⁵ Here, the proline oxidation activity of PltD was evaluated with PltE serving as a positive control. Proline oxidations assays were performed in a total volume of 100 μL containing 20 mM HEPES-Na (pH=7.9), 5 mM TCEP, 5 mM L-proline, 9 mM ATP, 10 mM MgCl₂, 50 μM FAD, 2.5 μM PltF, 75 μM holo-PltL, 10 μM PltD or PltE, and 10% glycerol at 30 °C for 6 h. Formation of pyrrolyl-*S*-PltL was not observed in assays containing PltD, while PltE demonstrated the ability to oxidize prolyl-*S*-PltL, as has been described previously.²⁵ Note that the intermediate prolyl-*S*-PltL is labile and is not detected in these assays, as has also been reported previously.²⁶

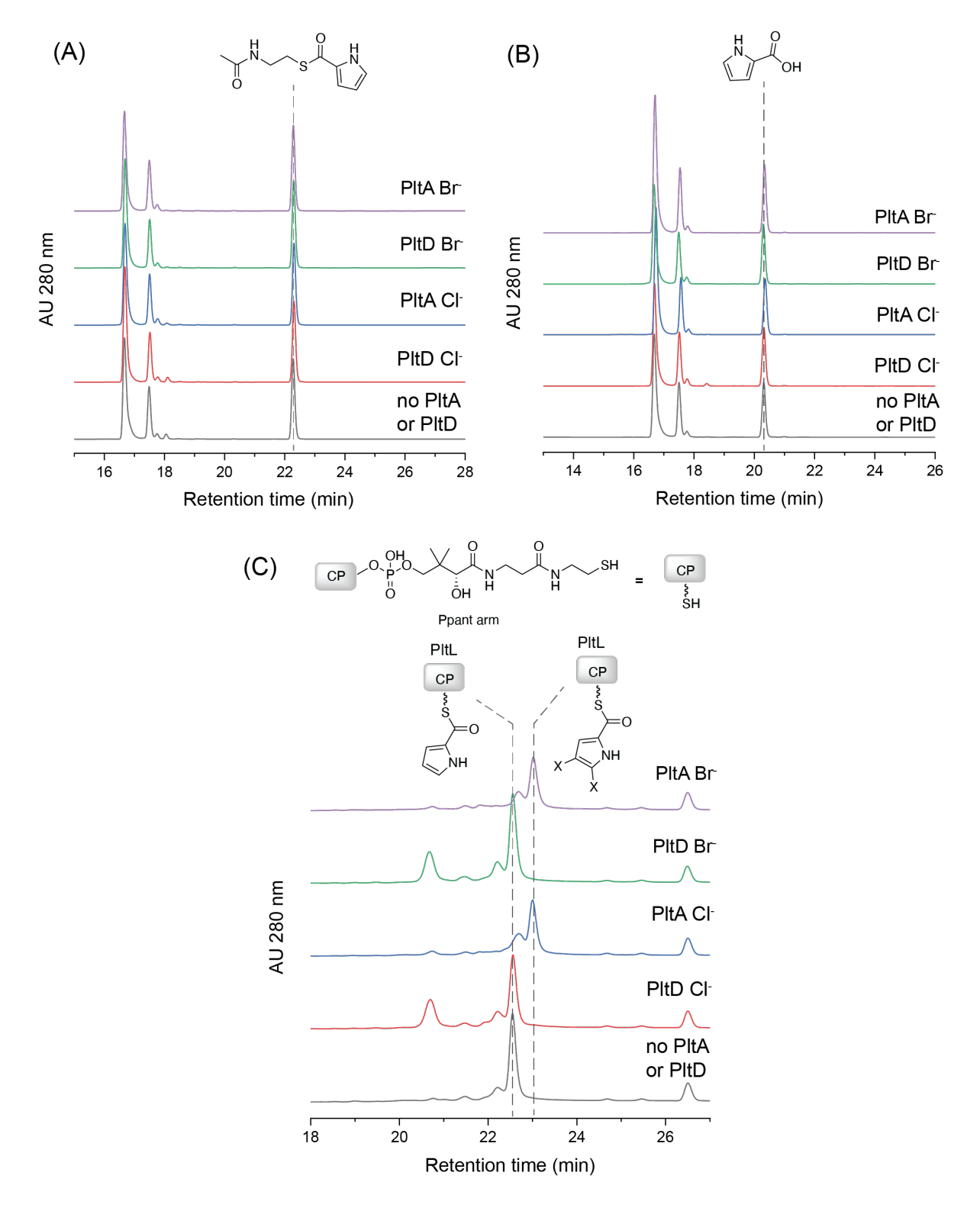


Figure S19: Lack of pyrrole halogenation activity for PltD. In pyoluteorin biosynthesis, the enzyme PltA serves to dichlorinate the pyrrolyl-*S*-PltL substrate.²⁷ Here, the halogenation activity of PltD was evaluated for a panel of pyrrolyl substrates with PltA acting as a positive control.

Assays were performed at 30 °C for 5 h, in a total volume of 100 μL containing 20 mM HEPES-Na (pH=7.9), 5 mM TCEP, 1 mM NAD⁺, 4 mM Na₂HPO₃, 0.1 mM FAD, 4 μM RebF, 4 μM PtdH, 200 mM KCl or KBr, 0.1 ng catalase, 20 μM PltD or PltA, 10% glycerol, together with (**A**) 0.2 mM pyrrolyl-*S*-N-acetylcysteamine (pyrrolyl-SNAC), (**B**) 0.2 mM pyrrole-2-carboxylic acid, or (**C**) 50 μM pyrrolyl-*S*-PltL substrates. No halogenated products were observed using pyrrolyl-SNAC or pyrrole-2-carboxylic acid substrates for PltA or PltD. For pyrrolyl-*S*-PltL, which is the physiological substrate for PltA, dichlorinated and dibrominated products were observed in the assay employing PltA, but no halogenated products were observed in assays employing PltD.

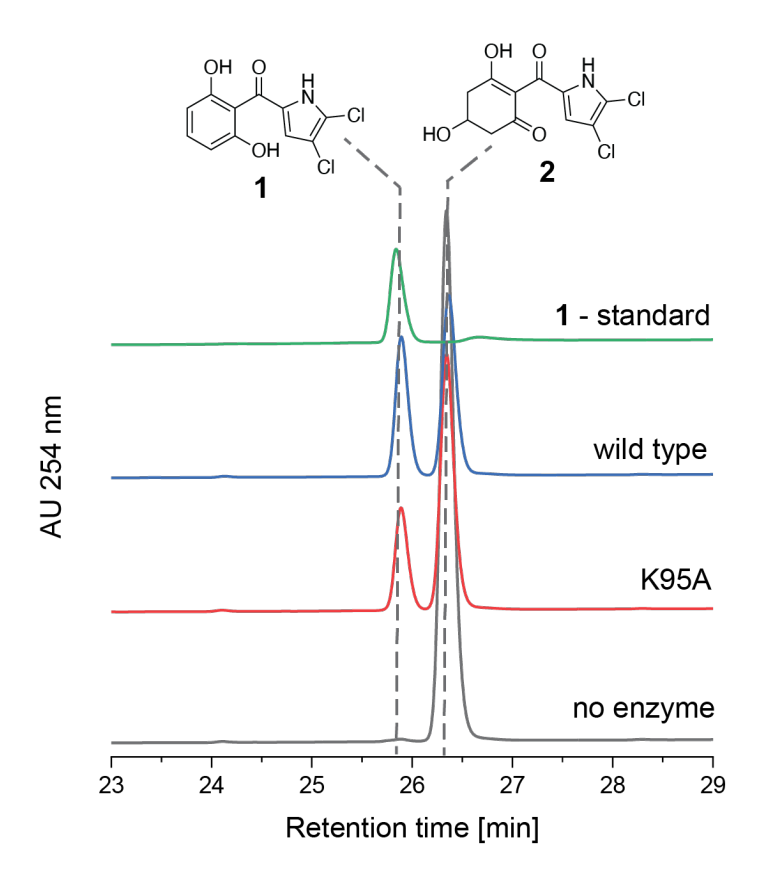


Figure S20: Activity of PltD K95A mutant enzyme compared with the wild type enzyme. Assays were performed in total volume of 100 μ L containing 0.25 mM **2**, 5 μ M PltD wild type or K95A mutant, and 400 potassium phosphate (pH=7.5) at 30 °C for 4 h. The K95A mutation did not abolish PltD activity.

SUPPLEMENTARY REFERENCES

- Yi, D.; Acharya, A.; Gumbart, J. C.; Gutekunst, W. R.; Agarwal, V., Gatekeeping ketosynthases dictate initiation of assembly line biosynthesis of pyrrolic polyketides. *J Am Chem Soc* 2021, 143 (20), 7617-7622.
- 2. Johannes, T. W.; Woodyer, R. D.; Zhao, H., Efficient regeneration of NADPH using an engineered phosphite dehydrogenase. *Biotechnol Bioeng* **2007**, *96* (1), 18-26.
- 3. Hughes, A. J.; Keatinge-Clay, A., Enzymatic extender unit generation for in vitro polyketide synthase reactions: structural and functional showcasing of *Streptomyces coelicolor* MatB. *Chem Biol* **2011**, *18* (2), 165-76.
- 4. Yan, Q.; Philmus, B.; Chang, J. H.; Loper, J. E., Novel mechanism of metabolic co-regulation coordinates the biosynthesis of secondary metabolites in *Pseudomonas protegens*. *eLife* **2017**, *6*, e22835.
- 5. Kong, L.-Y.; Cui, Q.; Jin, Z.; Xu, X.-H., Concise total synthesis of AB5046A and AB5046B. *Tetrahedron Lett* **2018**, *59* (18), 1705-1707.
- 6. Conradt, D.; Hermann, B.; Gerhardt, S.; Einsle, O.; Müller, M., Biocatalytic properties and structural analysis of phloroglucinol reductases. *Angew Chem Int Ed* **2016**, *55* (50), 15531-15534.
- 7. Cortes, J.; Haydock, S. F.; Roberts, G. A.; Bevitt, D. J.; Leadlay, P. F., An unusually large multifunctional polypeptide in the erythromycin-producing polyketide synthase of *Saccharopolyspora erythraea*. *Nature* **1990**, *348* (6297), 176-178.
- 8. Xue, Y.; Zhao, L.; Liu, H.-w.; Sherman, D. H., A gene cluster for macrolide antibiotic biosynthesis in *Streptomyces venezuelae*: architecture of metabolic diversity. *Proc Natl Acad Sci U S A* **1998,** *95* (21), 12111.
- 9. Caffrey, P.; Lynch, S.; Flood, E.; Finnan, S.; Oliynyk, M., Amphotericin biosynthesis in *Streptomyces nodosus*: deductions from analysis of polyketide synthase and late genes. *Chem Biol* **2001**, *8* (7), 713-723.
- 10. Ikeda, H.; Nonomiya, T.; Usami, M.; Ohta, T.; Ōmura, S., Organization of the biosynthetic gene cluster for the polyketide anthelmintic macrolide avermectin in *Streptomyces avermitilis*. *Proc Natl Acad Sci USA* **1999**, *96* (17), 9509.

- 11. Brautaset, T.; Sekurova, O. N.; Sletta, H.; Ellingsen, T. E.; Strøm, A. R.; Valla, S.; Zotchev, S. B., Biosynthesis of the polyene antifungal antibiotic nystatin in *Streptomyces noursei* ATCC 11455: analysis of the gene cluster and deduction of the biosynthetic pathway. *Chem Biol* **2000**, *7* (6), 395-403.
- 12. Fouces, R.; Mellado, E.; Díez, B.; Barredo, J. L., The tylosin biosynthetic cluster from *Streptomyces fradiae*: genetic organization of the left region. *Microbiology* **1999**, *145* (4), 855-868.
- 13. Keatinge-Clay, A. T., A tylosin ketoreductase reveals how chirality is determined in polyketides. *Chem Biol* **2007**, *14* (8), 898-908.
- 14. Keatinge-Clay, A., Crystal structure of the erythromycin polyketide synthase dehydratase. *J Mol Biol* **2008**, *384* (4), 941-953.
- 15. Akey, D. L.; Razelun, J. R.; Tehranisa, J.; Sherman, D. H.; Gerwick, W. H.; Smith, J. L., Crystal structures of dehydratase domains from the curacin polyketide biosynthetic pathway. *Structure* **2010**, *18* (1), 94-105.
- 16. Gay, D.; You, Y.-O.; Keatinge-Clay, A.; Cane, D. E., Structure and stereospecificity of the dehydratase domain from the terminal module of the rifamycin polyketide synthase. *Biochemistry* **2013**, *52* (49), 8916-8928.
- 17. Herbst, D. A.; Jakob, R. P.; Zähringer, F.; Maier, T., Mycocerosic acid synthase exemplifies the architecture of reducing polyketide synthases. *Nature* **2016**, *531* (7595), 533-537.
- 18. Shah, D. D.; You, Y.-O.; Cane, D. E., Stereospecific rormation of *E* and *Z*-disubstituted double bonds by dehydratase domains from modules 1 and 2 of the fostriecin polyketide synthase. *J Am Chem Soc* **2017**, *139* (40), 14322-14330.
- 19. Sung, K. H.; Berkhan, G.; Hollmann, T.; Wagner, L.; Blankenfeldt, W.; Hahn, F., Insights into the dual activity of a bifunctional dehydratase-cyclase domain. *Angew Chem Int Ed* **2018**, *57* (1), 343-347.
- Nowak-Thompson, B.; Chaney, N.; Wing, J. S.; Gould, S. J.; Loper, J. E., Characterization of the pyoluteorin biosynthetic gene cluster of *Pseudomonas fluorescens* Pf-5. *J Bacteriol* 1999, 181, 2166-2174.
- 21. Yamanaka, K.; Ryan, K. S.; Gulder, T. A. M.; Hughes, C. C.; Moore, B. S., Flavoenzyme-catalyzed atropo-selective N,C-bipyrrole homocoupling in marinopyrrole biosynthesis. *J Am Chem Soc* **2012**, *134* (30), 12434-12437.
- 22. Zhang, X.; Parry, R. J., Cloning and characterization of the pyrrolomycin biosynthetic gene clusters from *Actinosporangium vitaminophilum* ATCC 31673 and *Streptomyces* sp. strain UC 11065. *Antimicrob. Agents Chemother* **2007**, *51* (3), 946-57.

- 23. Flatt, P. M.; Wu, X.; Perry, S.; Mahmud, T., Genetic insights into pyralomicin biosynthesis in *Nonomuraea spiralis* IMC A-0156. *J Nat Prod* **2013**, *76* (5), 939-946.
- 24. Mori, S.; Pang, A. H.; Thamban Chandrika, N.; Garneau-Tsodikova, S.; Tsodikov, O. V., Unusual substrate and halide versatility of phenolic halogenase PltM. *Nat Commun* **2019**, *10* (1), 1255.
- 25. Thomas, M. G.; Burkart, M. D.; Walsh, C. T., Conversion of L-proline to pyrrolyl-2-carboxyl-S-PCP during undecylprodigiosin and pyoluteorin biosynthesis. *Chem Biol* **2002**, *9* (2), 171-84.
- 26. Garneau, S.; Dorrestein, P. C.; Kelleher, N. L.; Walsh, C. T., Characterization of the formation of the pyrrole moiety during clorobiocin and coumermycin A1 biosynthesis. *Biochemistry* **2005**, *44* (8), 2770-80.
- 27. Dorrestein, P. C.; Yeh, E.; Garneau-Tsodikova, S.; Kelleher, N. L.; Walsh, C. T., Dichlorination of a pyrrolyl-S-carrier protein by FADH₂-dependent halogenase PltA during pyoluteorin biosynthesis. *Proc Natl Acad Sci U S A* **2005**, *102* (39), 13843-8.